molecular pharmaceutics

Article

Efficient Click Synthesis of Protonize & Reduction-Sensitive Amphiphilic Small Molecule Prodrug Containing Camptothecin and Gemcitabine for Drug Self-Delivery System

Shuxiang Dong, Jinlin He, Yue Sun, Dian Li, Lei Li, Mingzu Zhang, and Peihong Ni

Mol. Pharmaceutics, **Just Accepted Manuscript** • DOI: 10.1021/acs.molpharmaceut.9b00349 • Publication Date (Web): 26 Jul 2019

Just Accepted

is published by the American Chemical Society. 1155 Sixteenth Street N.W., Washington, DC 20036

Efficient Click Synthesis of Protonized & Reduction-Sensitive Amphiphilic Small Molecule Prodrug Containing Camptothecin and Gemcitabine for Drug Self-Delivery System

Shuxiang Dong, Jinlin He, Yue Sun, Dian Li, Lei Li, Mingzu Zhang, and Peihong Ni*

College of Chemistry, Chemical Engineering and Materials Science, State and Local Joint Engineering Laboratory for Novel Functional Polymeric Materials, Jiangsu Key Laboratory of Advanced Functional Polymer Design and Application, Suzhou Key Laboratory of Macromolecular Design and Precision Synthesis, Soochow University, Suzhou 215123, P. R. China

Supporting Information:

ABSTRACT: Drug self-delivery systems consisting of small-molecule active drugs with nanoscale features for intracellular delivery without the need for additional polymeric carriers. In this work, we proposed a highly efficient strategy to fabricate protonized and reduction-responsive self-assembled drug nanoparticles from an amphiphilic small molecule Camptothecin-*ss*-*1,2,3-triazole*-Gemcitabine conjugate (abbreviated as CPT-*ss*-*triazole*-GEM) for combination chemotherapy, which was prepared via Cu(I)-catalyzed azide-alkyne cycloaddition (CuAAC) "click" reaction. In order to obtain this drug-*triazole*-drug conjugate, we first prepared a CPT derivate containing propargyl group linked with a disulfide group and a GEM derivate attached an azide group. Subsequently, the two kinds of modified drugs were connected together through CuAAC reaction between the alkynyl and azide groups to yield CPT-*ss*-*triazole*-GEM prodrug. The characterization of chemical structures of these intermediates and the final product were performed by ^{1}H NMR, FT-IR and LC/MS measurements. This amphiphilic small-molecule drug-*triazole*-drug conjugate displayed high drug loading content, that is, 36.0% of CPT and 27.2% of GEM. This kind of amphiphilic small-molecule prodrug could form spherical nanoparticles in aqueous solution in the absence of any other polymeric carriers, in which the hydrophobic CPT formed the core of the nanoparticles, while the hydrophilic GEM and protonated 1,2,3-triazole group yielded the shell. In the tumor microenvironment, the prodrug nanoparticles could release both pristine drugs simultaneously. Under the conditions of pH 7.4 and pH 7.4 plus 2 μM glutathione (GSH), the prodrug nanoparticles could maintain stable and only 7% of CPT was leaked. However, under a high GSH environment (pH 7.4 plus 10 mM GSH) with the same incubation time, the disulfide linkage would be dissociated and lead to about 34% of CPT release. The results of MTT test demonstrated that these prodrug nanoparticles showed higher cytotoxicity toward HepG2 cells than free CPT and free GEM in both 48 h and 72 h incubation. Both *in vitro* cellular uptake and flow cytometry results implied that these prodrug nanoparticles could be internalized by HepG2 cells with efficient drug release inside cells. The pharmacokinetics and tissue distribution of the prodrug showed a moderate half-life *in vivo* and the prodrug peak concentration in most of collected tissues appeared at 0.25 h after administration. In addition, CPT-*ss*-*triazole*-GEM prodrug could not cross blood-brain barrier. Even more important is that there is no accumulation in tissues and a rapid elimination of this small molecule prodrug could be achieved. In brief, this protonized and reduction-sensitive prodrug simultaneously binds both antitumor drugs and has good self-delivery behavior through the donor-acceptor interaction of H-bonding ligand, i.e. 1,2,3-triazole group. It provides a new method for the combined drug therapy.

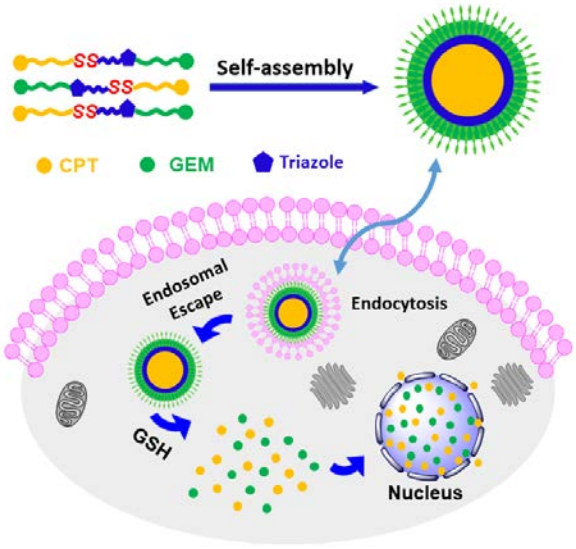

KEYWORDS: *Cancer therapy, Drug self-delivery systems, Small-molecule prodrug, Drug-drug cconjugate, Nano-medicine.*

INTRODUCTION

With the continuous advancement and development of nanotechnology, various strategies for cancer treatment have been broadened and deepened.[1] Some main routine treatments for tumors, for example, surgical intervention, radiation and chemotherapeutic drugs, have been widely used in clinic. Among them, chemotherapeutic drugs are most often used because of its potent efficiency, however they can cause severe adverse effect to the patients by killing normal cells. Therefore, more efforts have been focused on passively targeting carriers based on liposomes and polymers, or actively targeting carries, in which chemotherapeutic drugs are linked to a molecule that overexpresses antigen or receptor binding on target cells. Carrier-assistant drug delivery systems (DDSs) can overcome some shortcomings of conventional anticancer drugs, such as the limited solubility in physiological conditions, random distribution, rapid blood clearance and poor bioavailability.[2,3] However, there might be several limitations for these DDS systems, for example, low drug loading capacity, carrier-caused toxicity and immunogenicity, as well as complicated synthesis process.[4,5]

In contrast with carrier-assistant drug delivery systems, drug

Scheme 1. Synthetic pathways of the small-molecule prodrug CPT-*ss*-*triazole*-GEM and the donor-acceptor transformation mechanism of the protonized 1,2,3-triazole H-bonding ligand.

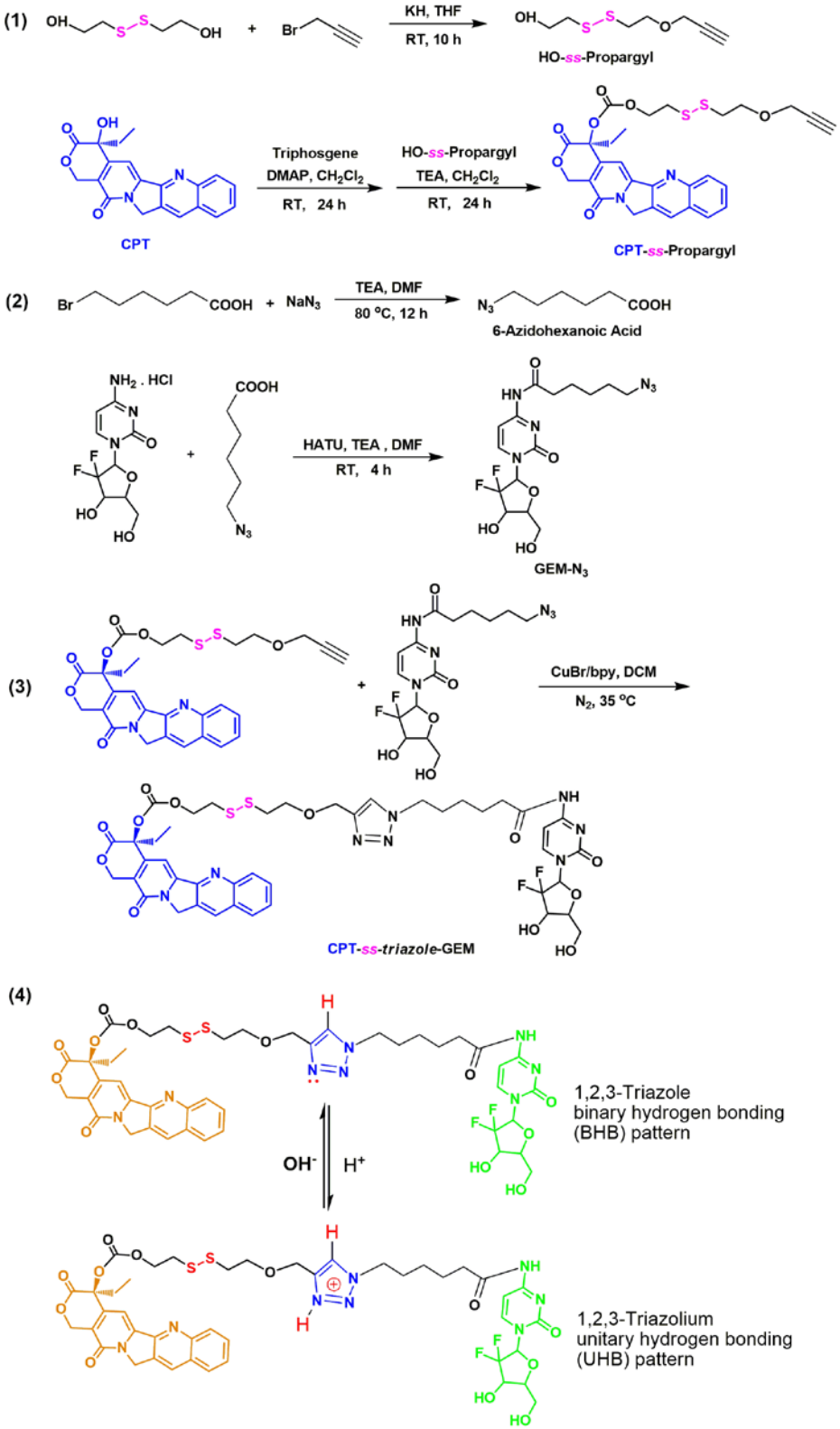

self-delivery systems (DSDSs) are a novel and highly effective paradigm of cancer treatment, in which the active drugs have nanoscale characteristics and can achieve intracellular delivery by themselves without the aid of any additional polymeric carriers.[6,7] By means of bottom-up self-assembly technique, the DSDSs attract the following attentions: (i) customizing nanoarchitectures that can protect drugs from leakage and realize the selective tumor accumulation through the enhanced permeation and retention (EPR) effect; (ii) potentially achieving high drug loading capacities without the incorporation of carriers; (iii) reducing the synthetic complexity of carriers, and (iv) avoiding the possible adverse effects induced by carriers.[8]

Camptothecin (CPT) is a widely used powerful anticancer drug which can induce the apoptosis of tumor cells through inhibiting type I DNA topoisomerase.[9-11] Gemcitabine (GEM) is also an antitumor therapeutic with a similar structure to Ara-Cs (Arabino Cytidines) and broad-spectrum in the treatment of various cancers[12] such as ovarian,[13] breast,[14] bladder,[15] small-cell lung cancer[16] and pancreatic cancer,[17] in combination chemotherapy treatment of leukemia and non-small-cell lung cancer.[18] Small molecule drug has precise chemical structure, which is critical to determine specific functionality for effective chemotherapy based on different drug delivery systems. Meanwhile, using nanomaterial self-assembly to accurately design nanomedicines with different biophysical and biochemical properties, the formulation can be optimized, for example, doxorubicin-tocopherol succinate prodrug,[19] irinotecan-chlorambucil,[20] chlorambucil-gemcitabine,[21] camptothecin-floxuridine,[22] gemcitabine-camptothecin conjugates,[23] and so on. Especially, Yan *et al.* reported an amphiphilic nanomedicine prepared from the small molecule drug-drug conjugates based on irinotecan (Ir) and chlorambucil (Cb). They found that this delivery system based on the small-molecule prodrug could drastically enhance the drug loading content and realize an excellent therapeutic property against cancer.[20]

Various stimuli-responsive linkers have been used for constructing drug conjugates, among which disulfide bond is particularly interesting since it keeps stable during blood circulation but can be rapidly cleaved by reductive thiols (such as glutathione) existed at enhanced levels in tumor regions.[24] In the past years, a lot of multifunctional disulfide-linked conjugate systems have been developed.[25] In addition, one of the advantages of small-molecule prodrugs is the potential for a high drug content of up to 100%, especially for amphiphilic drug-drug conjugates, in which one drug acts as the promoiety of the other.[26] Therefore, these co-drug conjugates can self-assembly to nanomedicine and provide a combination therapy that can enhance system potency.[27] Many studies on small-molecule disulfide-based prodrugs focus on bis(2-hydroxyethyl) disulfide compound since it can be easily built by esterification reaction[28-31] or amidation reaction.[32] Recently, the pioneering researches of CPT-*ss*-GEM nanoparticles based self-delivery system reported by Xu,[23] Yu[33] and Liang[34] have aroused much attention. For example, the amphiphilic small-molecule prodrug CPT-*ss*-GEM containing hydrophilic gemcitabine and hydrophobic camptothecin, which was connected by a disulfide linkage, can self-assemble into nanoparticles in water without the aid of additional carries. This prodrug nanoparticle displayed good stability and excellent blood compatibility *in vivo*. Moreover, it also achieved high drug loading capacities and avoided carrier-induced toxicity.

How to bond two different drugs is the key for the preparation of drug-drug conjugates. Some organic reactions can achieve such process, especially "click" chemistry, which is a highly efficient chemical reaction.[35-39] Cheng *et al.* have recently reported a facile way to manipulate the conformation of polypeptides by using the donor-acceptor interactions derived from the hydrogen-bonding ligands in pendant chains.[40] In detail, the 1,2,3-triazole group in the side chain of polypeptides serves as both H-bond donors and acceptors at neutral pH condition, which can disrupt the α-helical conformation of polypeptides. When the 1,2,3-triazol group was protonized at acidic condition, the resulting 1,2,3-triazolium group would not be H-bond acceptor and the α-helical structure of polypeptides was recovered. On the other hand, Hawker *et al.* found that the polar feature of the triazole nucleus could enhance the solubility of n-octyl derivatives, leading to complete dissolution of octyl-substituted polymers in methanol.[41]

Herein, we report on a new reduction-responsive small-molecule prodrug CPT-*ss*-*triazole*-GEM containing donor-acceptor interaction of H-bonding ligand, i.e. 1,2,3-triazole group, in which two anticancer drug derivatives, CPT-*ss*-Propargyl and GEM-N_3, was linked together by CuAAC "click" reaction as shown in Scheme 1. This amphiphilic prodrug is composed of hydrophobic CPT, hydrophilic GEM and protonated 1,2,3-triazole group, which can self-assembly nanoparticles and form a drug self-delivery system. To the best of our knowledge, this CPT derivative that links camptothecin (CPT) and propargyl via a disulfide bond has not been reported yet. Due to the amphiphilic and protonated feature, the small-molecule prodrug CPT-*ss*-*triazole*-GEM can self-assemble to form nanoparticles in water without the help of polymeric carriers. After entering into cancer cells by passive targeting, the dissociation of CPT-*ss*-*triazole*-GEM nanoparticles can be accelerated under the reductive microenvironment and acidic condition, thus resulting in a fast release of free CPT and GEM drugs. This work contributes a facile synthetic strategy for hydrophobic antineoplastic drug derivatives. It is well-known that many natural or synthetic hydrophobic anticancer drugs contain hydroxyl groups and/or amino groups,[42] such as PTX,[43,44] GEM[45,46] and DOX,[47,48] which have the potential to be modified into drug-*ss*-propargyl structures, and further to obtain drug-*ss*-*triazole*-drug conjugates via "click" chemistry.

EXPERIMENTAL SECTION

Provided in the Supporting Information Section are the detailed description of related materials, synthetic methods, characterization, self-assembly, in vitro and in vivo experiments.

RESULTS AND DISCUSSION

Synthesis of Small-Molecule Prodrug CPT-*ss*-*triazole*-GEM. The reduction-responsive small-molecule prodrug CPT-*ss*-*triazole*-GEM was prepared via the following procedures as illustrated in Scheme 1:

(1) Preparation of intermediate CPT-*ss*-Propargyl. CPT-*ss*-Propargyl was obtained by the esterification of CPT and 2-[(2-(prop-2-ynyloxy)ethyl)disulfanyl]ethanol, in which 4-(dimethylamino) pyridine (DMAP) worked as a catalyst and triphosgene provided an acyl group. The chemical structure of CPT-*ss*-Propargyl can be characterized by ^{1}H NMR and LC/MS analysis, respectively. The ^{1}H NMR spectrum in Figure 1 shows characteristic proton signals of the intermediate CPT-*ss*-Propargyl. By contrast with the ^{1}H NMR spectrum of CPT in Figure 1(A), the new chemical shifts appear at δ 2.88 ppm (peak d), δ 3.00 ppm (peak e), δ 3.41 ppm (peak a), δ 3.59 ppm (peak c), δ 4.08 ppm (peak b) and δ 4.33 ppm (peak f) in Figure 1(B), which can be attributed to the proton signals from 2-[(2-(prop-2-ynyloxy)ethyl)disulfanyl]ethanol. Moreover, the result of LC/MS

analysis shown in Figure S1 confirms the successful preparation of CPT-*ss*-Propargyl (LC/MS *m/z* calcd. for $C_{28}H_{26}N_2O_7S_2$ [M+1]: 567.3, found: 566.12.).

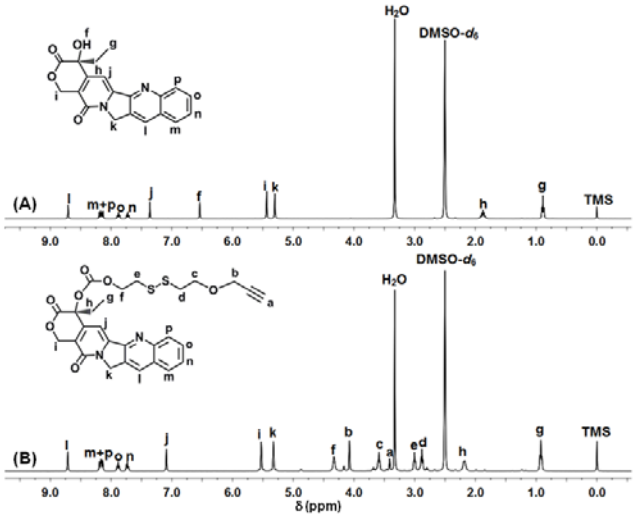

Figure 1. ^{1}H NMR spectra of (A) CPT and (B) CPT-*ss*-Propargyl (solvent: DMSO-d_6).

(2) Preparation of GEM-N$_3$. Firstly, 6-azidohexanoic acid was synthesized through a reaction of 6-bromohexanoic acid and sodium azide in DMF with 63% yield according to a previously published procedure.[48] Then, GEM-N$_3$ was prepared via an one-step amidation reaction between GEM·HCl and 6-azidohexanoic acid at room temperature with 58% yield in the presence of 1-[bis(dimethylamino)methylene]-1H-1,2,3-triazolo [4,5-b] pyridinium 3-oxid hexafluorophosphate (HATU) and triethylamine (TEA). FT-IR, ^{1}H NMR and LC/MS analyses were performed to confirm the chemical structure of GEM-N$_3$. Figure 2 shows the ^{1}H NMR spectra of GEM and GEM-N$_3$, from which all of the signals ascribed to the corresponding protons can be observed. Compared with the ^{1}H NMR spectrum of GEM in Figure 2(A), the new proton signals appear at δ 1.32 ppm (peak o and peak n), δ 1.55 ppm (peak k and peak m) and δ 2.42 ppm (peak j) in Figure 2(B), which can be ascribed to the protons of 6-azidohexanoic acid. Moreover, the peak a has shifted from δ 9.77 ppm to δ 11.0 ppm, indicating that the chemical structure of amine group has changed. The FT-IR spectra of GEM and GEM-N$_3$ are shown in Figure 3(A, B), from which one can observe that the peak at 2092 cm^{-1} in Figure 3(B), indicating the successful introduction of azide group into the GEM molecule. Moreover, the LC/MS analysis result in Figure S2 indicated that the found value (403.2) for $C_{15}H_{20}F_2N_6O_5$ [M+1] is close to the calculated value 402.15. All these results confirmed the successful preparation of GEM-N$_3$.

(3) Synthesis of CPT-*ss*-*triazole*-GEM. The final reduction-responsive small molecule prodrug CPT-*ss*-*triazole*-GEM was prepared via the CuAAC "click" reaction between CPT-*ss*-Propargyl and GEM-N$_3$. The ^{1}H NMR spectrum of CPT-*ss*-*triazole*-GEM is displayed in Figure 4, from which one can observe all the signals ascribed to the protons of CPT-*ss*-*triazole*-GEM. The FT-IR spectrum for CPT-*ss*-*triazole*-GEM is shown in Figure 3(C), in which the disappearance of the peak at 2092 cm^{-1} showed that the azide group was completely consumed. Furthermore, LC/MS analysis was adopted to confirm the structure (the test data LC/MS *m/z* calcd. for $C_{43}H_{46}F_2N_8O_{12}S_2$ [M+1]: 969.4, found: 968.26.), as shown in Figure S3. All these test data confirmed that the small-molecule prodrug CPT-*ss*-*triazole*-GEM has been synthesized successfully.

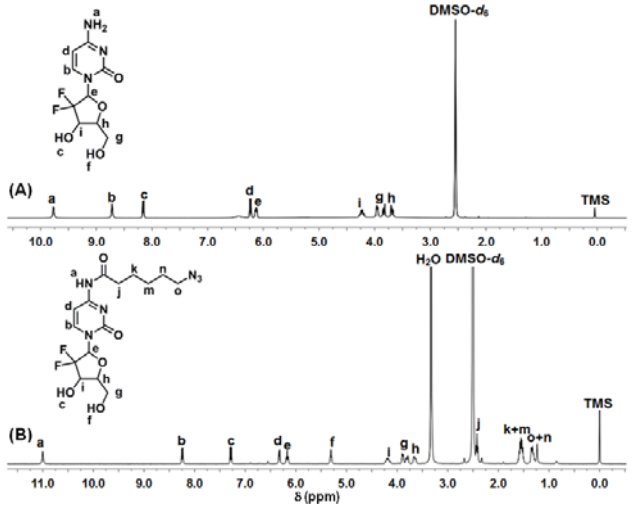

Figure 2. ^{1}H NMR spectra of (A) GEM and (B) GEM-N$_3$ (solvent: DMSO-d_6).

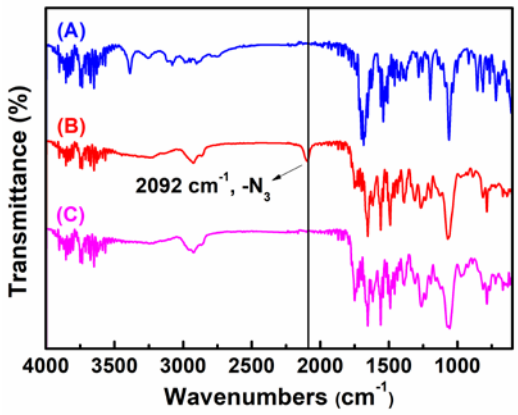

Figure 3. FT-IR spectra of (A) GEM, (B) GEM-N$_3$ and (C) CPT-*ss*-*triazole*-GEM.

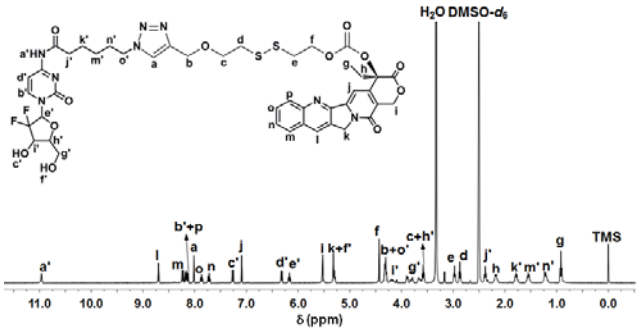

Figure 4. ^{1}H NMR spectrum of small-molecule prodrug CPT-*ss*-*triazole*-GEM (solvent: DMSO-d_6).

Self-Assembly Behavior of the Small-Molecule Prodrug CPT-*ss-triazole*-GEM. The amphiphilic small-molecule prodrug CPT-*ss-triazole*-GEM can form nanoparticles in aqueous solution with hydrophobic CPT moiety as the core and hydrophilic GEM part and protonated 1,2,3-triazole group as the shell after exceeding a critical concentration.[23] Unlike the self-assembly of amphiphilic polymeric prodrug in water, the small-molecule prodrug could be fabricated into nanoparticles by various mechanisms, including disulfide-induced mechanism,[26] intermolecular π-π stacking-induced assembly,[49,50] as well as lower crystallinity-induced mechanism.[51] In order to study the self-assembly behavior of this small-molecule prodrug CPT-*ss-triazole*-GEM, its critical aggregation concentration (CAC) value was measured by the pyrene fluorescence probe method. The impact of H-bonding pattern on the CPT-*ss-triazole*-GEM conformation is illustrated in Scheme 1(4). After being protonized, the resultant 1,2,3-triazolium groups displayed hydrophilic feature and lose the ability of acting as H-bond acceptors. As found in Figure 5, the CAC value was measured to be 0.0292 mg mL^{-1} from the fluorescence intensity ratio (I_3/I_1) as a function of the logarithm concentration of the CPT-*ss-triazole*-GEM prodrug. As a drug self-delivery system, the average particle size and size distribution are important parameters. Dynamic Light Scattering (DLS) and Transmission Electron Microscope (TEM) analyses were used to assess the properties of nanoparticle formed by the small-molecule prodrug. TEM image of the CPT-*ss-triazole*-GEM nanoparticles is displayed in Figure 6(A), from which we can find that these nanoparticles are mainly spherical and well dispersed. The corresponding particle size distribution curve measured by DLS analysis is shown in Figure 6(B) and exhibits unimodal distribution. A little difference in particle size between TEM and DLS results might be attributed to the easy aggregation of small-molecule prodrug. DLS measurement was further used to check the average diameter of CPT-*ss-triazole*-GEM nanoparticles during 6 days in three conditions (Milli-Q water, PBS, FBS) as shown in Figure 7, which indicated excellent stability in Milli-Q water and PBS over 6 days, but a little instability after 4 days in fetal bovine serum (FBS, 10 %).

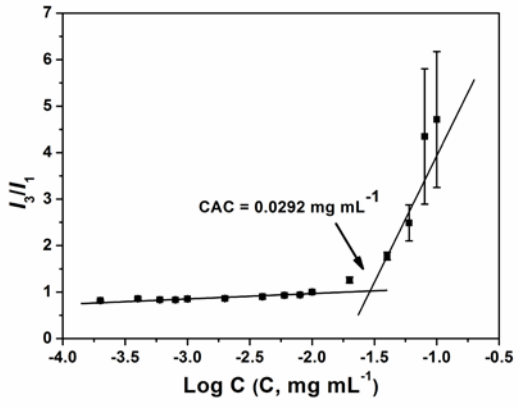

Figure 5. Intensity of the fluorescence emission spectrum of pyrene (I_3/I_1) as a function of logarithm concentration of the small-molecule prodrug CPT-*ss-triazole*-GEM in aqueous solution.

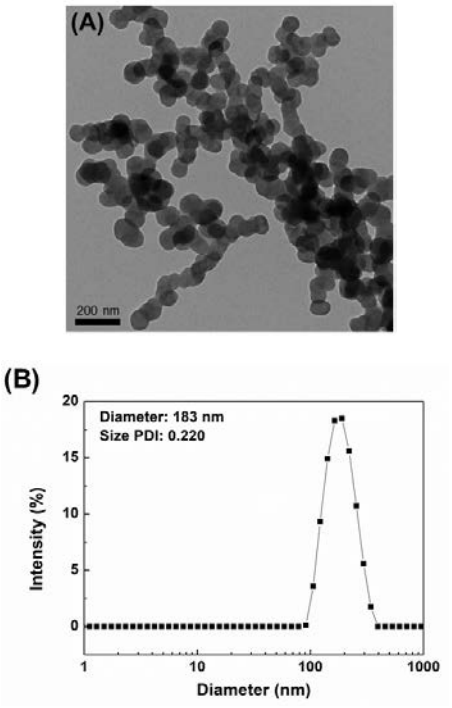

Figure 6. (A) TEM image of the CPT-*ss-triazole*-GEM prodrug nanoparticles with a scale bar of 200 nm; (B) the corresponding particles size distribution curve with a prodrug concentration of 0.1 mg mL^{-1}.

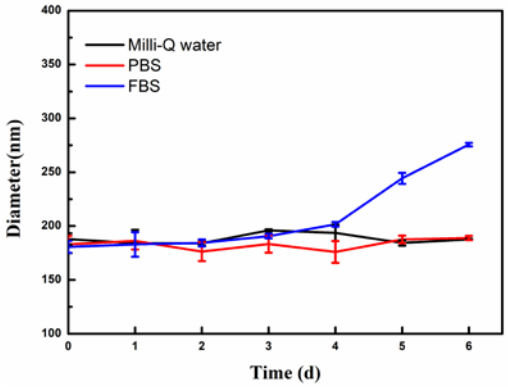

Figure 7. Particle size change of prodrug nanoparticles at different incubation time in three media: Milli-Q water, PBS and FBS (10%).

***In Vitro* Drug Release.** The reduction-sensitive property has been given after incorporating the disulfide carbonate linker into the prodrug. To further study the reduction-triggered dissociation of CPT-*ss-triazole*-GEM prodrug nanoparticles, *in vitro* drug release was measured in different conditions: (i) PB 7.4, (ii) PB 7.4 plus 2 μM GSH, and (iii) PB 7.4 plus 10 mM GSH. As shown in Figure 8(A), only a minimal CPT release (~7%) was measured after incubating for 100 h without GSH or with 2 μM GSH, which exhibited excellent stability in physiological condition. In comparison, the CPT release was greatly accelerated in the presence of 10 mM GSH within the same incubation time, and about 34% of CPT was released after incubating for 100 h. To predict the drug release property in tumorous region, we carry out the testing under a

more acidic condition in Figure 8(B), which was investigated in different conditions: (i) PB 5.0, (ii) PB 5.0 plus 2 mM GSH. Approximately 5% of CPT was released under PB 5.0 condition in contrast with about 38% of CPT was released under PB 5.0 plus 2 mM GSH condition. All these results indicated the favorable reduction-triggered drug release behavior, and these stimuli-responsive prodrug nanoparticles showed great potential in drug self-delivery system.

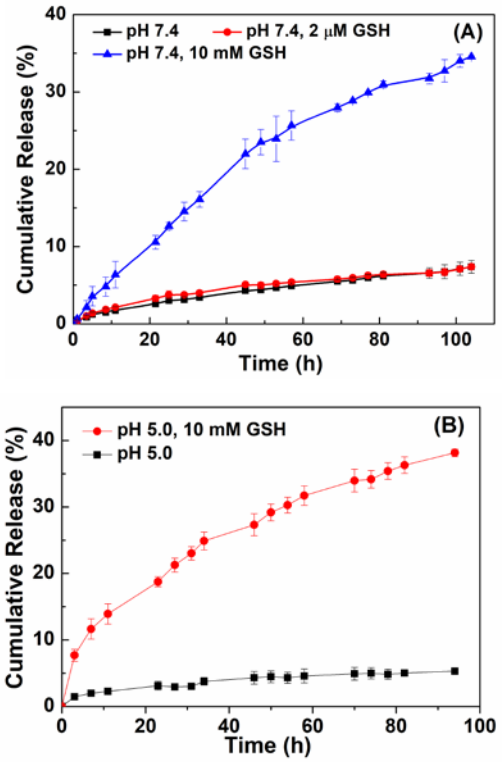

Figure 8. *In vitro* CPT release profiles from small-molecule prodrug CPT-*ss*-*triazole*-GEM nanoparticles in (A) PB 7.4 plus different GSH concentrations and (B) more acidic condition with different reductive GSH concentrations.

***In Vitro* Cytotoxicity.** According to our design, CPT-*ss*-*triazole*-GEM prodrug nanoparticles could be internalized into cells. In the microenvironment of tumors, CPT and GEM can be released into the nuclei almost simultaneously by triggering disulfide bond breakage. Therefore, it is anticipated that CPT-*ss*-*triazole*-GEM nanoparticles can exhibit antiproliferative activity against tumor cells. We utilized the MTT assay to investigated the cytotoxicity of different formulations against HepG2 cells using the MTT assay. Figure 9 shows the results of the cell viability of HepG2 cells, from which one can see that the cells gradually decreased with the increase of drug concentrations, indicating a dose-dependent anti-proliferative activity. Furthermore, at the same concentration, the CPT-*ss*-*triazole*-GEM prodrug nanoparticles were more cytotoxic than either free CPT or free GEM alone. The half maximal inhibitory concentration (IC_{50}) was also used to characterize the drug efficacy, which denotes the effectiveness of a substance in inhibiting a specific biological or biochemical function. The IC_{50} values of free CPT, free GEM and CPT-*ss*-*triazole*-GEM for HepG2 cells are about 1.38 mg L^{-1}, 1.61 mg L^{-1}, 1.39 mg L^{-1} in 24 h incubation shown in Figure 9(A); 2.61 mg L^{-1}, 16.48 mg L^{-1}, 0.41 mg L^{-1} in 48 h incubation shown in Figure 9(B); 0.56 mg L^{-1}, 0.64 mg L^{-1}, 0.10 mg L^{-1} in 72 h incubation shown in Figure 9(C), respectively. CPT-*ss*-*triazole*-GEM micelles exhibited a lower IC_{50} value than free CPT and free GEM, indicating a better antiproliferative effect.

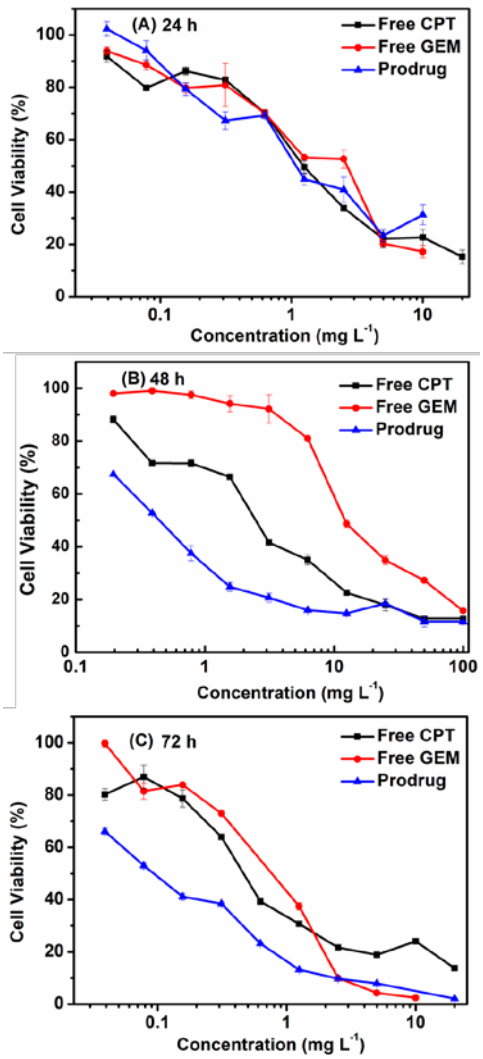

Figure 9. Cell viability of HepG2 cells treated with CPT-*ss*-*triazole*-GEM prodrug nanoparticles and free CPT or free GEM with different drug dosages for various incubation times: (A) 24 h, (B) 48 h and (C) 72 h. The IC_{50} values of free CPT, free GEM, and CPT-*ss*-*triazole*-GEM prodrug were determined by GraphPad Prism 5 software.

***In Vitro* Cellular Uptake.** The *in vitro* cellular uptake and intracellular drug release of CPT-*ss*-*triazole*-GEM prodrug nanoparticles incubated with HepG2 cells were monitored by a live cell imaging system. As displayed in Figure 10(A), the blue fluorescence of CPT was observed in the cytoplasm of HepG2 cells after incubation with CPT-*ss*-*triazole*-GEM prodrug nanoparticles for 4.5 h, indicating the successful internalization of the prodrug nanoparticles and efficient CPT release inside HepG2 cells. In addition, with the increasing incubation time from 4.5 h to 24 h, the observed CPT fluorescence inside cells was greatly enhanced. By contrast, as shown in Figure 10(B), free CPT exhibited relatively less fluorescence in HepG2 cells with the same incubation time possibly because of the different cellular internalization mecha-

nisms between free drug (diffusion) and prodrug nanoparticles (endocytosis). These results implied that the prodrug nanoparticles could be internalized by HepG2 cells with efficient drug release. To further detect the fluorescence intensity of HepG2 cells incubated with free CPT and CPT-*ss-triazole*-GEM prodrug nanoparticles for fixed time intervals (4.5 h, 8.5 h, and 24 h), flow cytometry was adopted to observe the fluorescence intensity of HepG2 cells. The result is shown in Figure 11, the relative geometrical mean fluorescence intensities of HepG2 cells with the prodrug nanoparticles increased with the increasing time. Notably, there is stronger CPT fluorescence intensity at 24 h than those of them at 4.5 h, indicating that the uptake of CPT-*ss-triazole*-GEM prodrug nanoparticles was time-dependent property.

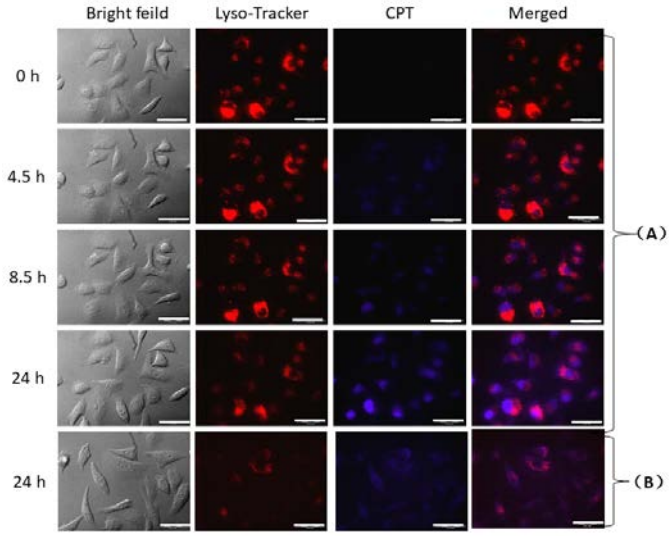

Figure 10. Fluorescence images of HepG2 cells incubated with (A) CPT-*ss-triazole*-GEM nanoparticles and (B) free CPT for different times. The CPT dosage was 17.98 mg L^{-1}. For each panel, images from left to right show bright field images, cell nuclei stained by Lyso-Tracker Red (red), CPT (blue) and overlays of the blue and red images. The scale bars are 50 μm in all images.

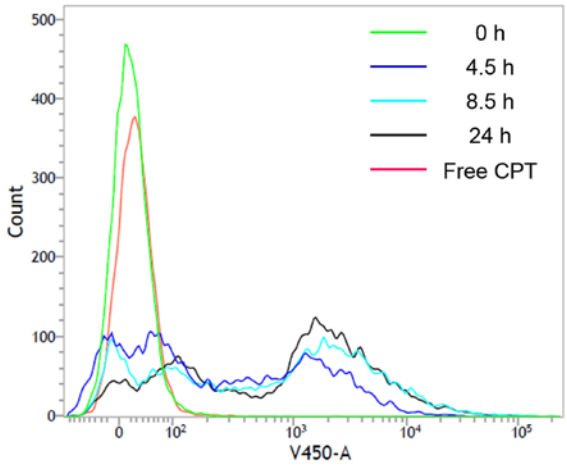

Figure 11. Flow cytometry curves of HepG2 cells treated with CPT-*ss-triazole*-GEM prodrug nanoparticles for different times (4.5 h, 8.5 h, and 24 h) with a certain concentration of CPT (17.98 mg L^{-1}).

Pharmacokinetics and Distribution of CPT-*ss-triazole*-GEM Prodrug. To determine the pharmacokinetics of CPT-*ss-triazole*-GEM prodrug in rat, we used the UHPLC-MS/MS method. CPT-*ss-triazole*-GEM prodrug was delivered via intravenous, respectively. The blood samples were collected from tail at indicated time after dosing. The mean concentration-time curve is shown in Figure 12. The pharmacokinetic parameters were figured out and summarized in Table 1. The results showed that CPT-*ss-triazole*-GEM prodrug has a moderate half-life *in vivo*.

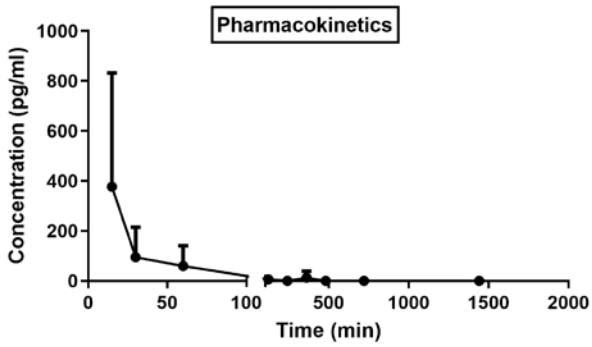

Figure 12. The pharmacokinetic curve of CPT-*ss-triazole*-GEM prodrug. The mice were intravenously administration of CPT-*ss-triazole*-GEM prodrug at dose of 5 mg kg^{-1}. The blood samples were collected at the indicated time point. The validated UHPLC-MS/MS assay was employed to determine the concentration of CPT-*ss-triazole*-GEM prodrug. The concentration time curve was plotted, n = 6.

Table 1. Pharmacokinetic parameters of CPT-*ss-triazole*-GEM prodrug administrated through intravenous.

***i.v.* 5mg /kg**	
AUC(0-t) (μg/L*h)	402.525 ± 496.57
AUC(0-∞) (μg/L*h)	402.525 ± 496.57
MRT(0-t) (h)	0.589 ± 0.378
MRT(0-∞) (h)	0.59± 0.38
t1/2z (h)	1.294 ± 1.271
Tmax (h)	0.25 ± 0.00
CLz (L/h/kg)	71.62 ± 89.28
Vz (L/kg)	313.716 ± 439.992
Cmax (μg/L)	376.764 ± 455.515
C0 (μg/L)	1635.169 ± 1760.459

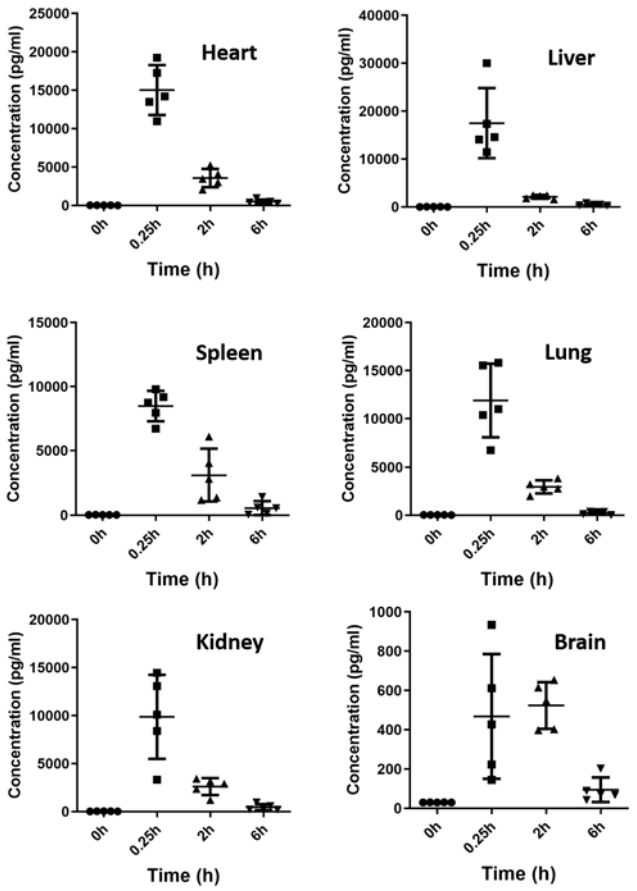

Figure 13. Tissue distribution of CPT-*ss-triazole*-GEM prodrug. The mice were intravenously administration of CPT-*ss-triazole*-GEM prodrug at dose of 5 mg kg^{-1}. The blood, heart, liver, spleen, lung, kidney, brain samples were collected at 0.25h. The validated UHPLC-MS/MS assay was employed to determine the concentration of CPT-*ss-triazole*-GEM in each organ. The concentration time curve was plotted, n = 6.

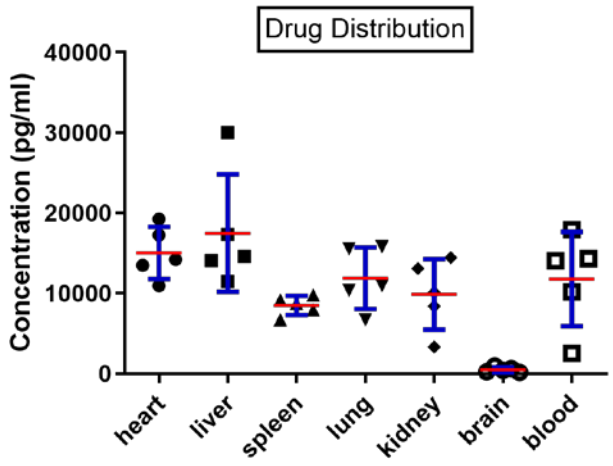

Figure 14. The distribution study of CPT-*ss-triazole*-GEM prodrug. The mice were intravenously administration of CPT-*ss-triazole*-GEM prodrug at dose of 5 mg kg^{-1}. The blood, heart, liver, spleen, lung, kidney, brain samples were collected at 0.25 h. The validated UHPLC-MS/MS assay was used to determine the concentration of CPT-*ss-triazole*-GEM prodrug in each organ. The concentration time curve was plotted, n = 6.

The tissue distribution of CPT-*ss-triazole*-GEM prodrug *in vivo* was further assessed in rat and the results were showed in Figure 13 and Figure 14. The results showed that the peak concentration of CPT-*ss-triazole*-GEM prodrug in most of collected tissues appeared at 0.25 h after administration and CPT-*ss-triazole*-GEM prodrug could not cross blood-brain barrier (Figure 13). Moreover, the he tissue area under the curve from time zero to 6 h was in the following order: liver > heart > kidney > lung > spleen > brain (Figure 14). As shown in Figure 14, the concentration levels in liver and heart were much higher than those in other tissues, illustrating that liver and heart are the main target organs of CPT-*ss-triazole*-GEM prodrug. Over time, the main trend of the prodrug concentration of icariin in all tissues was reduced, and the concentration dropped very quickly at 2h after administration, suggesting no accumulation in tissues and a rapid elimination of this compound.

CONCLUSIONS

In summary, a novel reduction-responsive small-molecule prodrug CPT-*ss-triazole*-GEM has been successfully synthesized using the CPT-*ss*-Propargyl and GEM-N_3 via the CuAAC "click" reaction. We utilized donor-acceptor interactions H-bonding ligand and 1,2,3-triazole group between two small molecule drugs (CPT and GEM). Because of its amphiphilic feature, the small-molecule prodrug CPT-*ss-triazole*-GEM can self-assemble to form spherical nanoparticles in water in the absence of additional polymeric carriers, in which the hydrophobic CPT constituted the core of nanoparticles, while the hydrophilic GEM and protonated 1,2,3-triazole groups yielded the shell. This amphiphilic small molecule drug-drug conjugate (CPT-*ss-triazole*-GEM) showed high drug loading capacity, 36.0% of CPT and 27.2% of GEM. The size of nanoparticle is about 180 nm, which could simultaneously release fixed dosage of the two drugs free CPT and free GEM in cancer cells. The cumulative release is approximate 34%. The results of MTT assay demonstrated that the prodrug nanoparticles exhibited higher cytotoxicity (IC_{50}: 0.41 mg L^{-1}) against HepG2 cells than free CPT (IC_{50}: 2.61 mg L^{-1}) and free GEM (IC_{50}: 16.48 mg L^{-1}) in 48 h incubation. Also, in 72 h incubation, the prodrug exhibited higher cytotoxicity (IC_{50}: 0.10 mg L^{-1}) against HepG2 cells than free CPT (IC_{50}: 0.56 mg L^{-1}) and free GEM (IC_{50}: 0.64 mg L^{-1}). Both cellular uptake and flow cytometry results implied that the prodrug could be internalized by HepG2 cells with efficient drug release from the nanoparticles. The pharmacokinetics and tissue distribution of the prodrug showed a moderate half-life *in vivo* and the peak concentration of CPT-*ss-triazole*-GEM prodrug in most of collected tissues appeared at 0.25 h after administration. Moreover, CPT-*ss-triazole*-GEM prodrug could not cross blood-brain barrier. All these results suggest no accumulation in tissues and a rapid elimination of this small-molecule prodrug. This protonizable and reduction-sensitive prodrug binds two antitumor drugs simultaneously through disulfide linker and possess the characteristics of low toxicity, reduction-responsiveness, and effective tumor therapy.

■ ASSOCIATED CONTENT

Supporting Information

Detailed description of related materials, synthesis and characterization details. LC/MS spectra of CPT-*ss*-Propargyl, GEM-N_3, and CPT-*ss*-triazole-GEM. LC/MS spectra of CPT-*ss*-Propargyl, GEM-N_3, and CPT-*ss-triazole*-GEM.

■ AUTHOR INFORMATION

Corresponding Author

* Tel: +86 512 65882047; E-mail: phni@suda.edu.cn

ORCID

Jinlin He: 0000-0003-3533-2905

Peihong Ni: 0000-0003-4572-3213

Notes

The authors declare no competing financial interest.

■ ACKNOWLEDGMENTS

The authors are grateful for the financial supports from the National Natural Science Foundation of China (21374066), the Major Program of the Natural Science Project of Jiangsu Higher Education Institutions (15KJA150007), Natural Science Foundation of Jiangsu Province (BK20171212), and a project funded by the Priority Academic Program Development (PAPD) of Jiangsu Higher Education Institutions. We thank Professor Jian Liu (FUNSOM, Soochow University) for his valuable help in the cell-related tests. We are also very grateful to Professor Xiaohui Zheng of Wenzhou Medical University for her help in supplementing *in vivo* testing.

■ REFERENCES

(1) Fan, W. P.; Yung, B.; Huang, P.; Chen, X. Y. Nanotechnology for multimodal synergistic cancer therapy. *Chem. Rev.* **2017**, *117*, 13566-13638.
(2) Peer, D.; Karp, J. M.; Hong, S.; Farokhzad, O. C.; Margalit, R.;Langer, R. Nanocarriers as an emerging platform for cancer therapy. *Nat. Nanotechnology* **2007**, *2*, 751-760.
(3) Min, Y. Z.; Caster, J. M.; Eblan, M. J.; Wang, A. Z. Clinical translation of nanomedicine. *Chem. Rev.* **2015**, *115*, 11147-11190.
(4) Cho, K.; Wang, X.; Nie, S.; Chen, Z.; Shin, D. M. Therapeutic nanoparticles for drug delivery in cancer. *Clin. Cancer Res.* **2008**, *14*, 1310-1316.
(5) Shen, Y.; Jin, E.; Zhang, B.; Murphy, C. J.; Sui, M.; Zhao, J.; Wang, J.; Tang, J.; Fan, M.; Kirk, E. V.; Murdoch, W. J. Prodrugs forming high drug loading multifunctional nanocapsules for intracellular cancer drug delivery. *J. Am. Chem. Soc.* **2010**, *132*, 4259-4265.
(6) Duan, X.; Chen, H.; Fan, L.; Kong, J. Drug self-assembled delivery system with dual responsiveness for cancer chemotherapy. *ACS Biomater. Sci. Eng.* **2016**, *2*, 2347-2354.
(7) Qin, S. Y.; Zhang, A. Q.; Cheng, S. X.; Rong, L.; Zhang, X. Z. Drug self-delivery systems for cancer therapy. *Biomaterials* **2017**, *112*, 234-247.
(8) Duan, X.; Chen, J.; Wu, Y.; Wu, S.; Shao, D.; Kong, J. Drug self-delivery systems based on hyperbranched polyprodrugs towards tumor therapy. *Chem. Asian J.* **2018**, *13*, 939-943.
(9) Zhang, X. L.; Zhang, M. K.; Wang, M. Q.; Peng, H.; Hua, Q.; Ma, L. H.; Wang, B. Y.; Wei, H. Facile fabrication of 10-Hydroxycamptothecin-Backboned amphiphilic polyprodrug with precisely tailored drug loading content for controlled release. *Bioconjugate Chem.* **2018**, *29*, 2239-2247.
(10) Thomas, C. J.; Rahier, N. J.; Hecht, S. M. Camptothecin: current perspectives. *Bioorg. Med. Chem.* **2004**, *12*, 1585-1604.
(11) Krishnan, P.; Rajan, M.; Kumari, S.; Sakinah, S.; Priya, S. P.; Amira, F.; Danjuma, L.; Ling, M. P.; Fakurazi, S.; Arulselvan, P.; Higuchi, A.; Arumugam, R.; Alarfaj, A. A.; Munusamy, M. A.; Hamat, R. A.; Benelli, G.; Murugan, K.; Kumar, S. S. Efficiency of newly formulated camptothecin with β-cyclodextrin-EDTA-Fe_3O_4 nanoparticle-conjugated nanocarriers as an anti-colon cancer (HT29) drug. *Sci. Rep.* **2017**, *7*, 10962.
(12) Pasut, G.; Canal, F.; Via, L. D.; Arpicco, S.; Veronese, F. M.; Schiavon, O. Antitumoral activity of PEG-gemcitabine prodrugs targeted by folic acid. *J. Control. Release* **2008**, *127*, 239-248.
(13) Fruscella, E.; Gallo, D.; Ferrandina, G.; D'Agostino, G.; Scambia, G. Gemcitabine: current role and future options in the treatment of ovarian cancer. *Crit. Rev. Oncol./Hematol.* **2003**, *48*, 81-88.
(14) Pérez-Manga, G.; Lluch, A.; Alba, E.; Moreno-Nogueira, J. A.; Palomero, M.; Garcia-Conde, J.; Khayat, D.; Rivelles, N. () Gemcitabine in combination with doxorubicin in advanced breast cancer: Final results of a phase II pharmacokinetic trial. *J. Clin. Oncol.* **2000**, *18*, 2545-2552.
(15) Sternberg, C. N. Gemcitabine in bladder cancer. *Semin. Oncol.* **2000**, *27 (1suppl 2)*, 31-39.
(16) Hoang, T.; Kim, K. M.; Jaslowski, A.; Koch, P.; Beatty, P.; McGovern, J.; Quisumbing, M.; Shapiro, G.; Witte, R.; Schiller, J. H. Phase II study of secondline gemcitabine in sensitive or refractory small cell lung cancer. *Lung Cancer* **2003**, *42*, 97-102.
(17) Carmichael, J.; Fink, U.; Russell, R. C. G.; Spittle, M. F.; Harris, A. L.; Spiessi, G.;; Blatter, J. Phase II study of gemcitabine in patients with advanced pancreatic cancer. *Br. J. Cancer* **1996**, *73*, 101-105.
(18) Crinò, L.; Calandri, C. Gemzar platinum combinations: phase III trials in non-small cell lung cancer. *Lung Cancer* **2002**, *38 (suppl 2)*, S9-S12.
(19) Duhem, N.; Danhier, F.; Pourcelle, V.; Schumers, J.-M.; Bertrand, O.; LeDuff, C. C. S.; Hoeppener, S.; Schubert, U. S.; Gohy J.-F. O.; Marchand-Brynaert, J. Self-assembling doxorubicin-tocopherol succinate prodrug as a new drug delivery system: Synthesis, characterization, and in vitro and in vivo anticancer activity. *Bioconjugate Chem.* **2014**, *25*, 72-81.
(20) Huang, P.; Wang, D. L.; Su, Y.; Huang, W.; Zhou, Y. F.; Cui, D. X.; Zhu, X. Y.; Yan, D. Y. Combination of small molecule prodrug and nanodrug delivery: Amphiphilic drug–drug conjugate for cancer therapy. *J. Am. Chem. Soc.* **2014**, *136*, 11748-11756.
(21) Fan, M.; Liang, X.; Li, Z.; Wang, H.; Yang, D.; Shi, B. Chlorambucil gemcitabine conjugate nanomedicine for cancer therapy. *Eur. J. Pharm. Sci.* **2015**, *79*, 20-26.
(22) Hu, M. X.; Huang, P.; Wang, Y.; Su, Y.; Zhou, L. Z.; Zhu X. Y.; Yan, D. Y. Synergistic combination chemotherapy of camptothecin and floxuridine through self-assembly of amphiphilic drug-drug Conjugate. *Bioconjugate Chem.* **2015**, *26*, 2497-2506.
(23) Hou, M. L.;, Xue, P.; Gao, Y. E.; Ma, X. Q.; Bai, S., Kang, Y. J.; Xu, Z. G. Gemcitabine-camptothecin conjugates: a hybrid prodrug for controlled drug release and synergistic therapeutics. *Biomater. Sci.* **2017**, *5*, 1889-1897.
(24) Lee, M. H.; Yang, Z.; Lim, C. W.; Lee, Y. H.; Dongbang, S.; Kang, C.; Kim, J. S. Disulfide-cleavage-triggered chemosensors and their biological applications. *Chem. Rev.* **2013**, *113*, 5071-5109.
(25) Lee, M. H.; Sessler, J. L.; Kim, J. S. Disulfide-based multifunctional conjugates for targeted theranostic drug delivery. *Acc. Chem. Res.* **2015**, *48*, 2935-2946.
(26) Wang, Y. J.; Liu, D.; Zheng, Q. C.; Zhao, Q.; Zhang, H. J.; Ma, Y.; Fallon, J. K.; Fu, Q.; Haynes, M. T.; Lin, G. M.; Zhang, R.;

Wang, D.; Yang, X. G.; Zhao, L. X.; He, Z. G.; Liu, F. Disulfide bond bridge insertion turns hydrophobic anticancer prodrugs into self-assembled nanomedicines. *Nano Lett.* **2014**, *14*, 5577-5583.
(27) Cheetham, A. G.; Chakroun, R. W.; Ma, W.; Cui, H. G. Self-assembling prodrugs. *Chem. Soc. Rev.* **2017**, *46*, 6638-6663.
(28) Wu, X. M.; Sun, X. R.; Guo, Z. Q.; Tang, J. B.; Shen, Y. Q.; James, T. D.; Tian, H.; Zhu, W. H. In vivo and in situ tracking cancer chemotherapy by highly photostable NIR fluorescent theranostic prodrug. *J. Am. Chem. Soc.* **2014**, *136*, 3579-3588.
(29) Pei, Q.; Hu, X. L.; Li, Z. S.; Xie, Z. G.; Jing, X. B. Small molecular nanomedicines made from a camptothecin dimer containing a disulfide bond. *RSC Adv.* **2015**, *5*, 81499-81501.
(30) Liu, Y.; Pei, Q.; Chen, L.; Li, Z. S.; Xie, Z. G. Reduction-responsive fluorescence off-on BODIPY-camptothecin conjugates for self-reporting drug release. *J. Mater. Chem. B* **2016**, *4*, 2332-2337.
(31) Zhang, F. W.; Zhu, G. Z.; Jacobson, O.; Liu, Y.; Chen, K.; Yu, G. C.; Ni, Q. Q.; Fan. J.; Yang, Z.; Xu, F.; Fu, X.; Wang, Z.; Ma, Y.; Niu, G.; Zhao, X. B.; Chen X. Y. Transformative nanomedicine of an amphiphilic camptothecin prodrug for long circulation and high tumor uptake in cancer therapy. *ACS Nano* **2017**, *11*, 8838-8848.
(32) Santra, S.; Kaittanis, C.; Santiesteban, O. J.; Perez, J. M. Cell-specific, activatable, and theranostic prodrug for dual-targeted cancer imaging and therapy. *J. Am. Chem. Soc.* **2011**, *133*, 16680-16688.
(33) Xu, Y. Y.; Huang, Y. S.; Zhang, X. W.; Lu, W.; Yu, J. H.; Liu, S. Y. Carrier-free Janus nano-prodrug based on camptothecin and gemcitabine: Reduction-triggered drug release and synergistic in vitro antiproliferative effect in multiple cancer cells. *Inter. J. Pharm.* **2018**, *550*, 45-56.
(34) Zhang, W.; Wen, Y.; He, D. X.; Wang, Y. F.; L, X. L.; Li, C.; Liang, X. J. Near-infrared AIEgens as transformers to enhance tumor treatment efficacy with controllable self-assembled redox-responsive carrier-free nanodrug. Biomaterials **2019**, *193*, 12-21
(35) Kolb, H. C.; Finn, M. G.; Sharpless, K. B. Click chemistry: Diverse chemical function from a few good reactions. *Angew. Chem., Int. Ed.* **2001**, *40*, 2004-2021.
(36) Liang, L. Y.; Astruc, D. The copper (I)-catalyzed alkyne-azide cycloaddition (CuAAC) “click” reaction and its applications. An overview. *Coord. Chem. Rev.* **2011**, *255*, 2933-2945.
(37) Hänni, K. D.; Leigh, D. A. The application of CuAAC 'click' chemistry to catenane and rotaxane synthesis. *Chem. Soc. Rev.* **2010**, *39*, 1240-1251.
(38) Bicak, T. C.; Gicevicˇius, M.; Gokoglan, T. C.; Yilmaz, G.; Ramanavicius, A.; Toppare, L.; Yagci, Y. Simultaneous and sequential synthesis of polyaniline-*g*-poly(ethylene glycol) by combination of oxidative polymerization and CuAAC click chemistry: A water-soluble instant response glucose biosensor material. *Macromolecules* **2017**, *50*, 1824-1831.
(39) Such, G. K.; Johnston, A. P. R.; Liang, K.; Caruso, F. Synthesis and functionalization of nanoengineered materials using click chemistry. *Prog. Polym. Sci.* **2012**, *37*, 985-1003.
(40) Song, Z.; Mansbach, R. A.; He, H.; Shih K. C.; Baumgartner, R.; Zheng, N.; Ba, X.;, Huang, Y.; Mani, D.; Liu, Y.; Lin, Y.; Nieh, M. P.; Ferguson, A. L.; Yin L. C.; Cheng, J. J. Modulation of polypeptide conformation through donor–acceptor transformation of side-chain hydrogen bonding ligands. *Nat. Commun.* **2017**, *8*, 92.
(41) Thibault, R. J.; Takizawa, K.; Lowenheilm, P.; Helms, B.; Mynar, J. L.; Frechet, J. M. J.; Hawker, C. J. *J. Am. Chem. Soc.* **2006**, *128*, 12084-12085.
(42) Seidi, F.; Jenjob, R.; Crespy, D. Designing smart polymer conjugates for controlled release of payloads. *Chem. Rev.* **2018**, *118*, 3965-4036.
(43) Huizing, M. T.; Misser, V. H. S.; Pieters, R. C.; ten Bokkel Huinink, W. W.; Veenhof, C. H. N.; Vermorken, J. B.; Pinedo, H. M.; Beijnen, J. H. Taxanes: A new class of antitumor agents. *Cancer Invest.* **1995**, *13*, 381-404.
(44) Wall, M. E.; Wani, M. C. Camptothecin and taxol: Discovery to clinic-Thirteenth Bruce F. Cain memorial award lecture. *Cancer Res.* **1995**, *55*, 753-760.
(45) Pollera C. F.; Ceribelli, A.; Crecco, M.; Oliva, C.; Calabresi, F. Prolonged infusion gemcitabine: a clinical phase I study at low- (300 mg/m^2) and high-dose (875 mg/m^2) levels. *Investig New Drugs* **1997**, *15*, 115-121.
(46) Abbruzzese, J. L.; Grunewald, R.; Weeks, E. A.; Gravel, D.; Adams, T.; Nowak, B.; Mineishi, S.; Tarassoff, P.; Satterlee, W.; Raber, M. N. A phase I clinical, plasma, and cellular pharmacology study of gemcitabine. *J. Clin. Oncol.* **1991**, *9*, 491-498.
(47) Berry, G.; Billingham, M.; Alderman, E.; Richardson, P.; Torti, F.; Lum, B.; Patek, A.; Martin, F. J. The use of cardiac biopsy to demonstrate reduced cardiotoxicity in AIDS Kaposi's sarcoma patients treated with pegylated liposomal doxorubicin. *Ann. Oncol.* **1998**, *9*, 711-716.
(48) Chen, X. J.; Parelkar, S. S.; Henchey, E.; Schneider, S.; Emrick, T. PolyMPC-doxorubicin prodrugs. *Bioconjugate Chem.* **2012**, *23*, 1753-1763.
(49) Luo, C.; Sun, J.; Liu, D.; Sun, B. J.; Miao, L.; Musetti, S.; Li, J.; Han, X. P.; Du, Y. Q.; Li, L.; Huang, L.; He, Z. G. Self-assembled redox dual-responsive prodrug-nanosystem formed by single thioether-bridged paclitaxel-fatty acid conjugate for cancer chemotherapy. *Nano Lett.* **2016**, *16*, 5401-5408.
(50) Luo, C.; Sun, J.; Sun, B. J.; Liu, D.; Miao, L.; Goodwin, T. J.; Huang, L.; He, Z. G. Facile fabrication of tumor redox-sensitive nanoassemblies of small-molecule oleate prodrug as potent chemotherapeutic nanomedicine. *Small* **2016**, *12*, 6353-6362.
(51) Zhong, T.; Yao, X.; Zhang, S.; Guo,Y.; Duan, X. C.; Ren, W.; Huang, D.; Yin, Y. F.; Zhang, X. A self-assembling nanomedicine of conjugated linoleic acid-paclitaxel conjugate (CLA-PTX) with higher drug loading and carrier-free characteristic. *Sci. Rep.* **2016**, *6*, 36614.

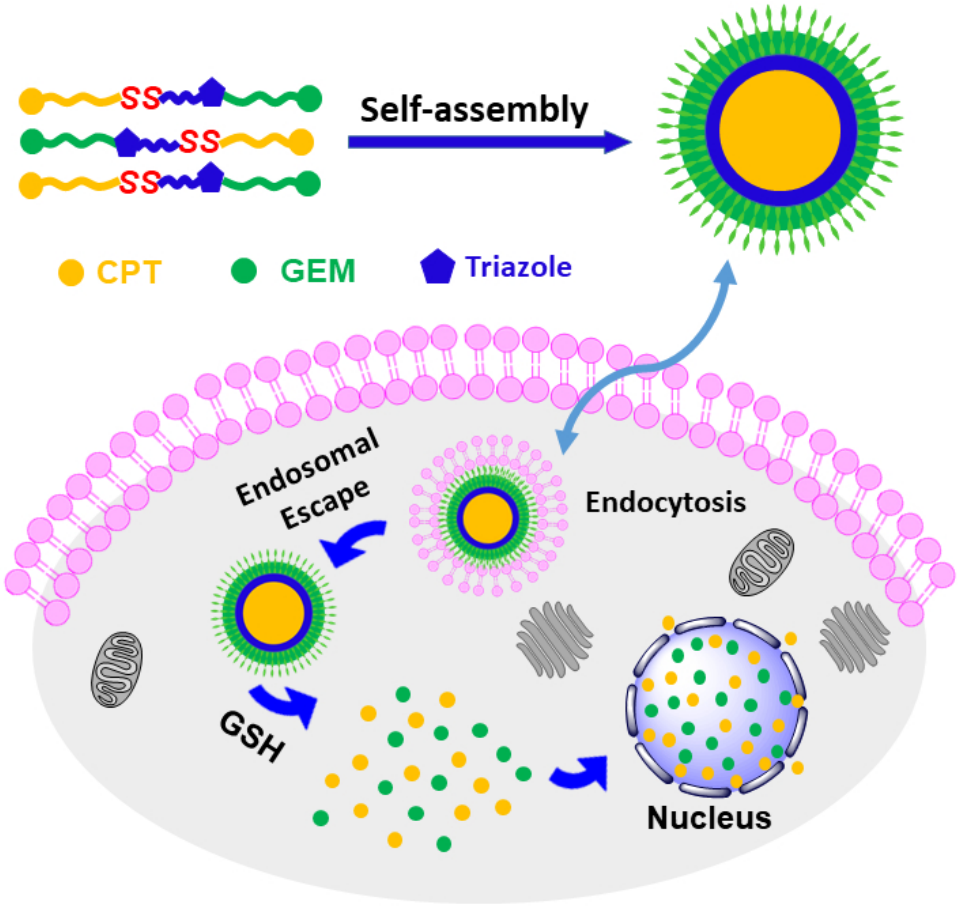

Schematic illustration of the Protonize & Reduction-Sensitive Amphiphilic Small Molecule Prodrug CPT-*ss*-*triazole*-GEM for the intracellularly triggered release of drugs in the tumor microenvironment.

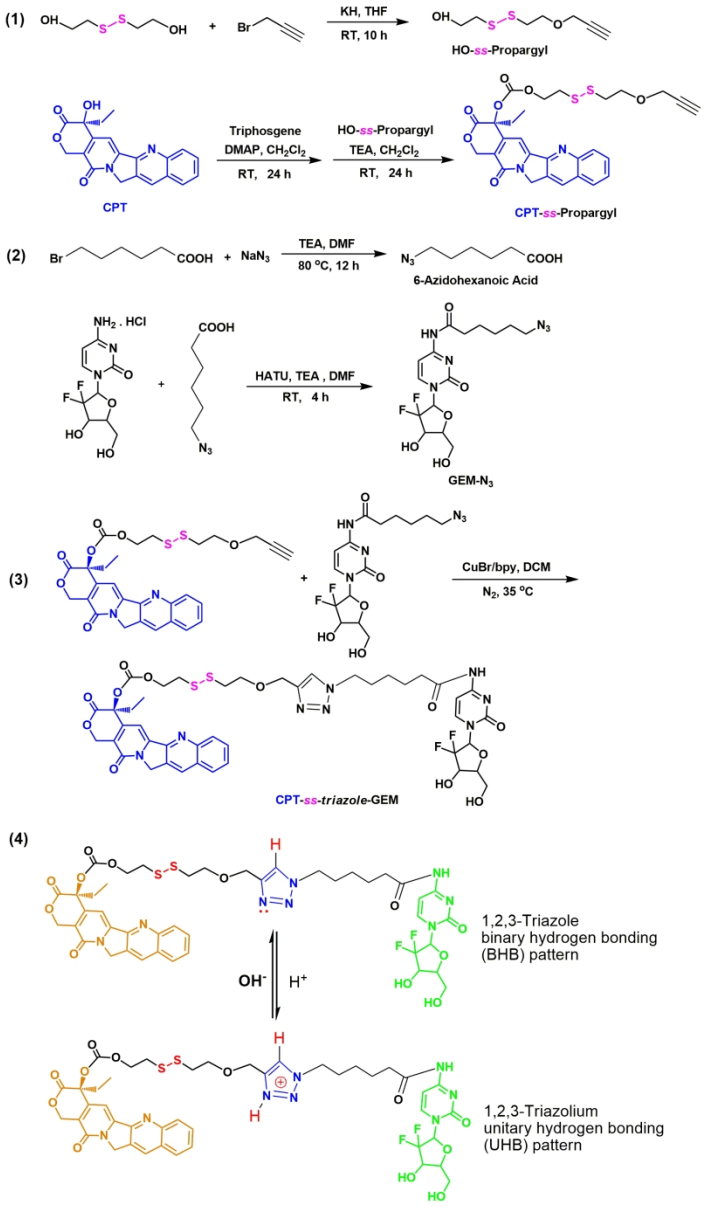

Scheme 1. Synthetic pathways of the small-molecule prodrug CPT-ss-triazole-GEM and the donor-acceptor transformation mechanism of
the protonized 1,2,3-triazole H-bonding ligand.

154x263mm (300 x 300 DPI)

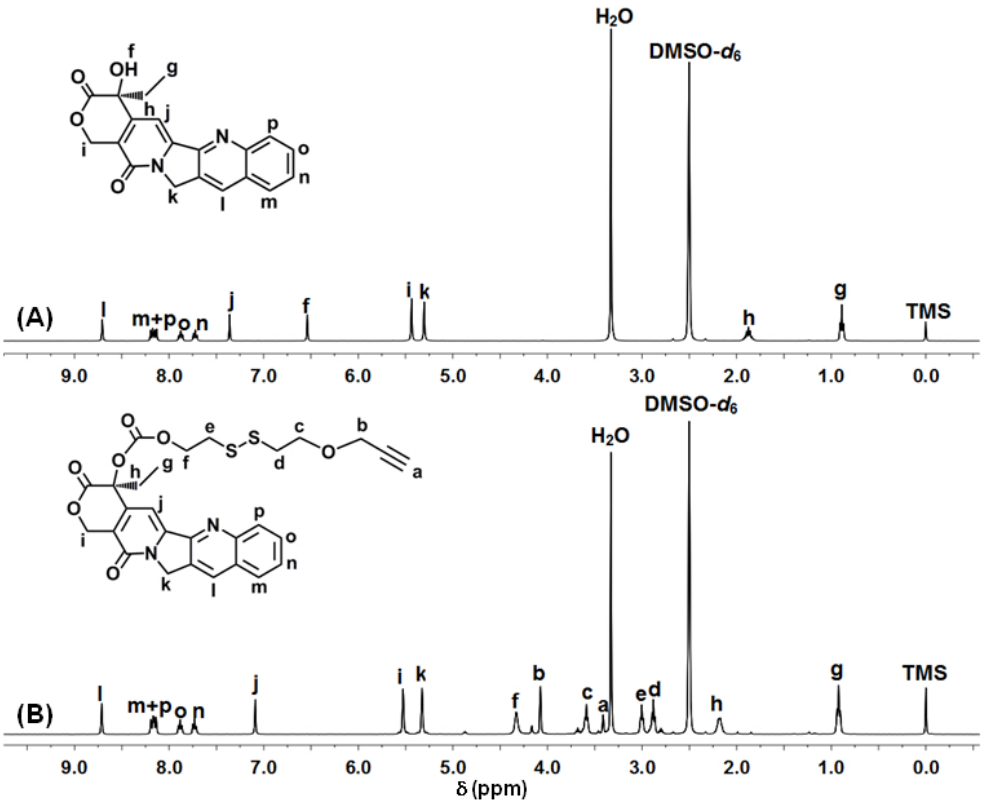

Figure 1. ^{1}H NMR spectra of (A) CPT and (B) CPT-*ss*-Propargyl. (solvent: DMSO-d_6)

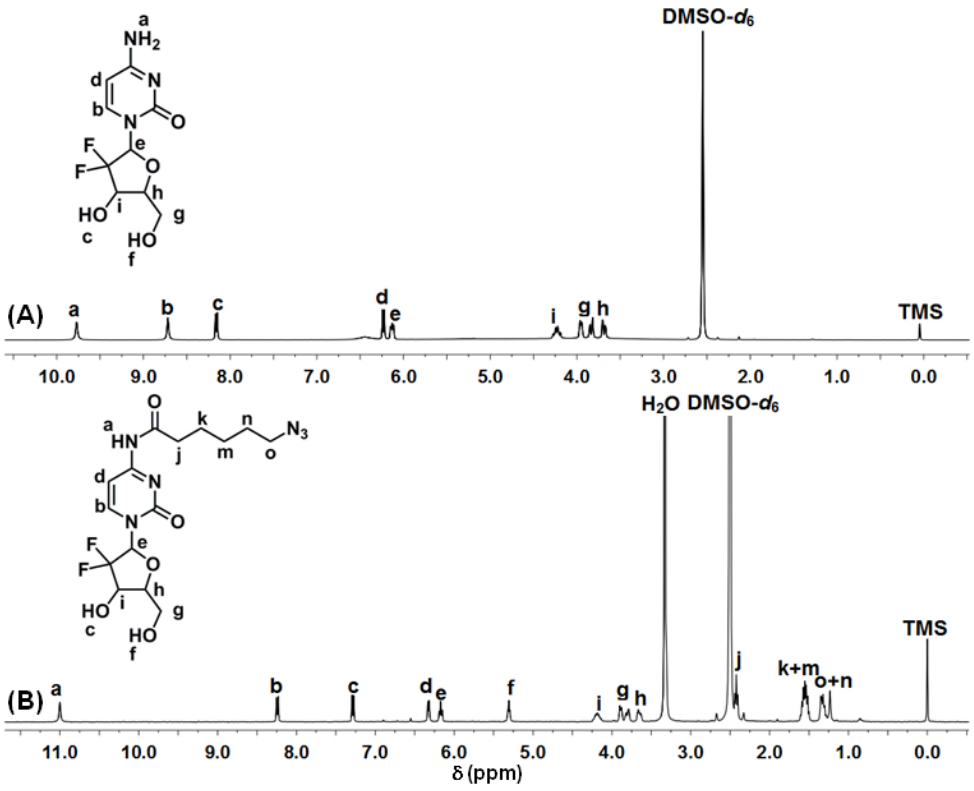

Figure 2. ^{1}H NMR spectra of (A) GEM and (B) GEM-N_3. (solvent: DMSO-d_6)

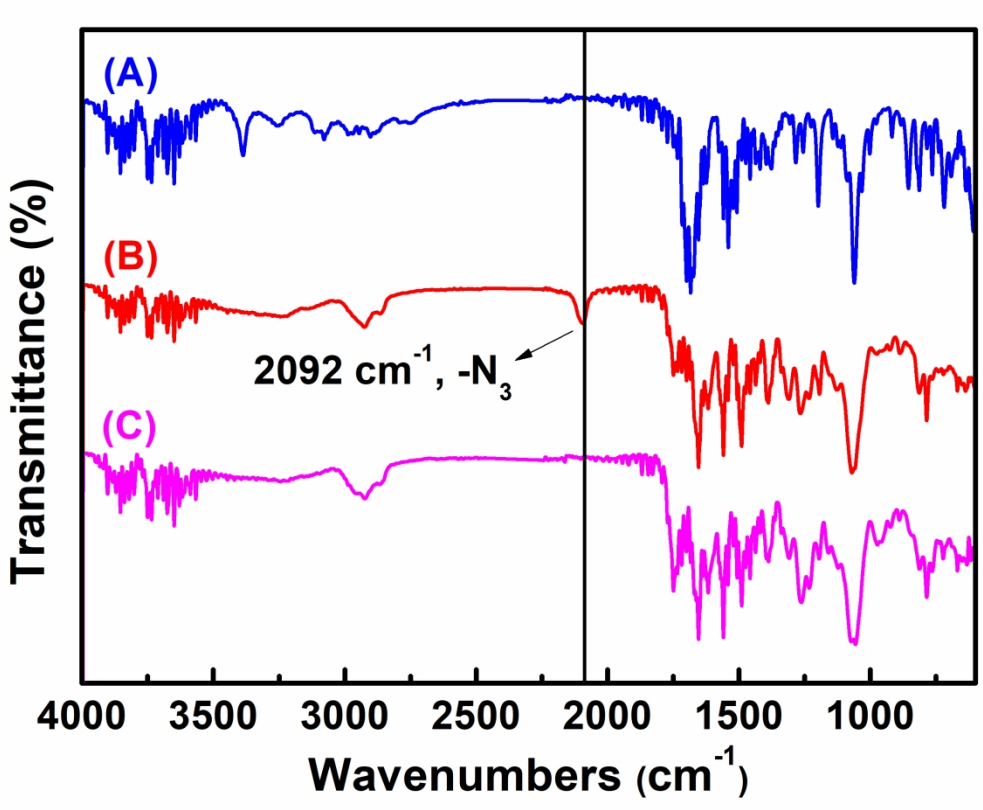

Figure 3. FT-IR spectra of (A) GEM, (B) GEM-N_3 and (C) CPT-*ss-triazole*-GEM.

688x559mm (96 x 96 DPI)

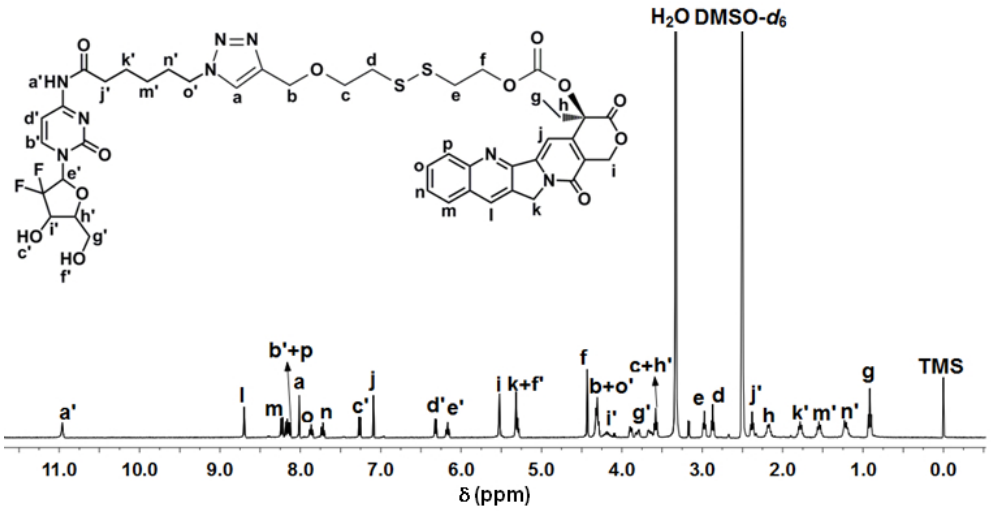

Figure 4. ^{1}H NMR spectrum of small-molecule prodrug CPT-*ss*-*triazole*-GEM. (solvent: DMSO-d_6)

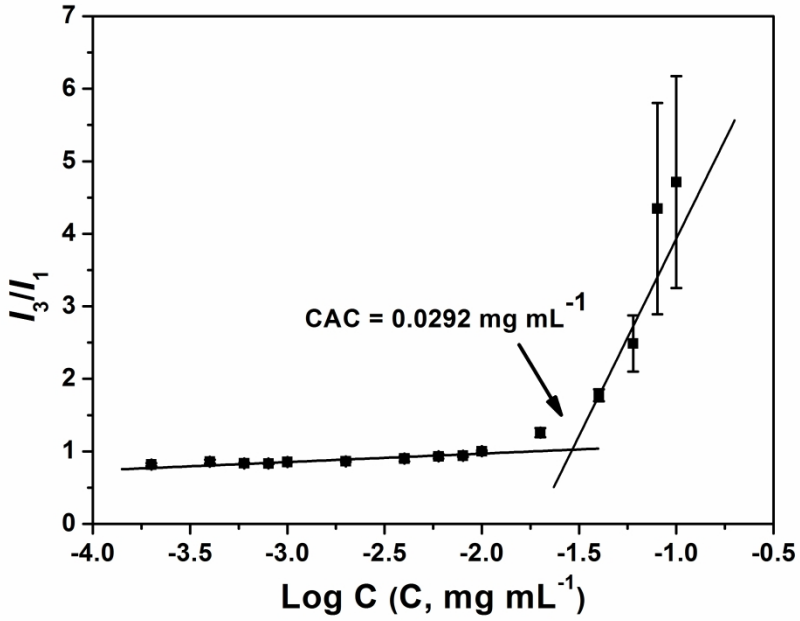

Figure 5. Intensity of the fluorescence emission spectrum of pyrene (I_3/I_1) as a function of logarithm concentration of the small-molecule prodrug CPT-*ss-triazole*-GEM prodrug in aqueous solution.

296x209mm (300 x 300 DPI)

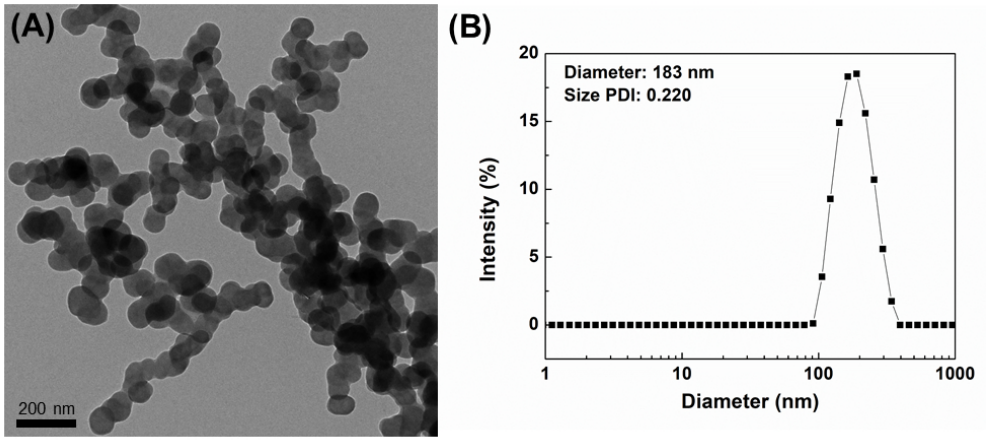

Figure 6. (A) TEM image of the CPT-*ss*-*triazole*-GEM prodrug nanoparticles with a scale bar of 200 nm; (B) the corresponding particles size distribution curve with a prodrug concentration of 0.1 mg mL^{-1}.

261x120mm (96 x 96 DPI)

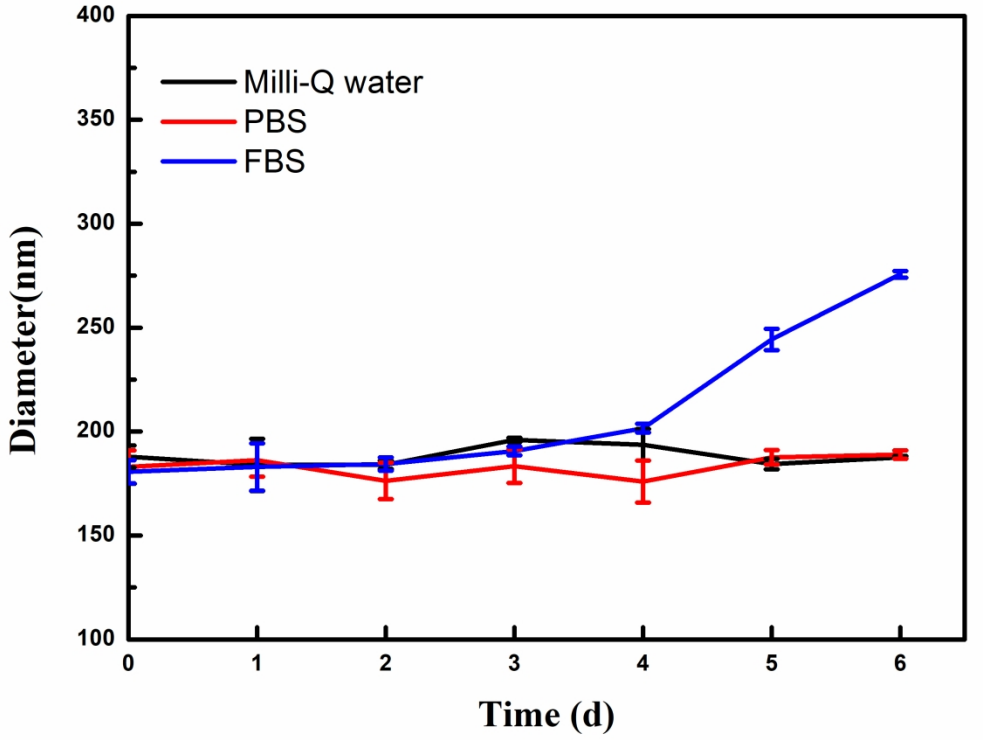

Figure 7. Particle size change of prodrug nanoparticles at different incubation time in three media: Milli-Q water, PBS and FBS (10%).

755x561mm (96 x 96 DPI)

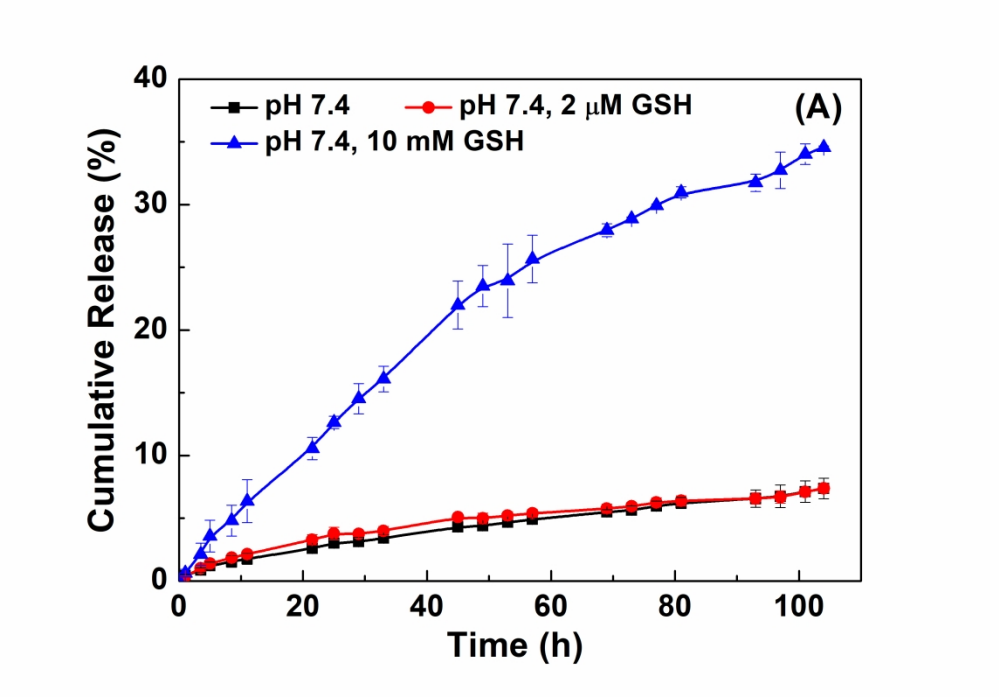

288x201mm (300 x 300 DPI)

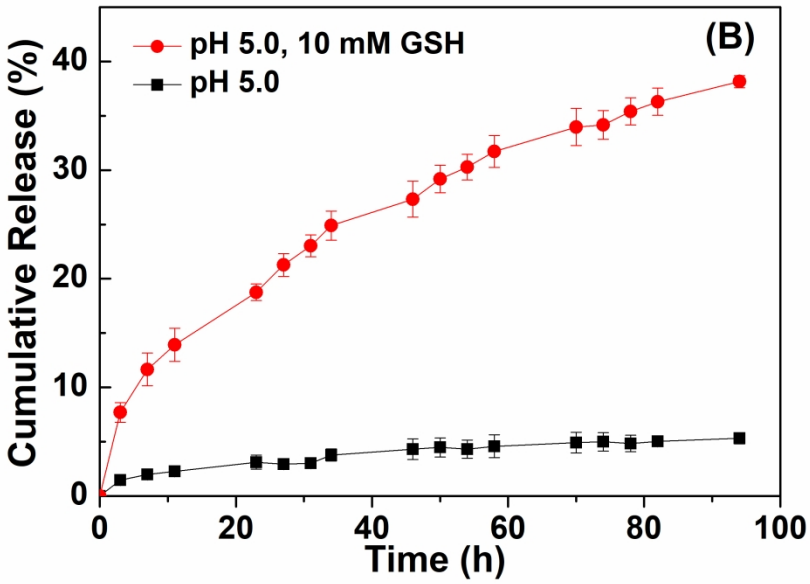

In vitro CPT release profiles from small-molecule prodrug CPT-*ss*-*triazole*-GEM nanoparticles in (A) PB 7.4 plus different GSH concentrations and (B) more acidic condition with different reductive GSH concentrations.

271x184mm (300 x 300 DPI)

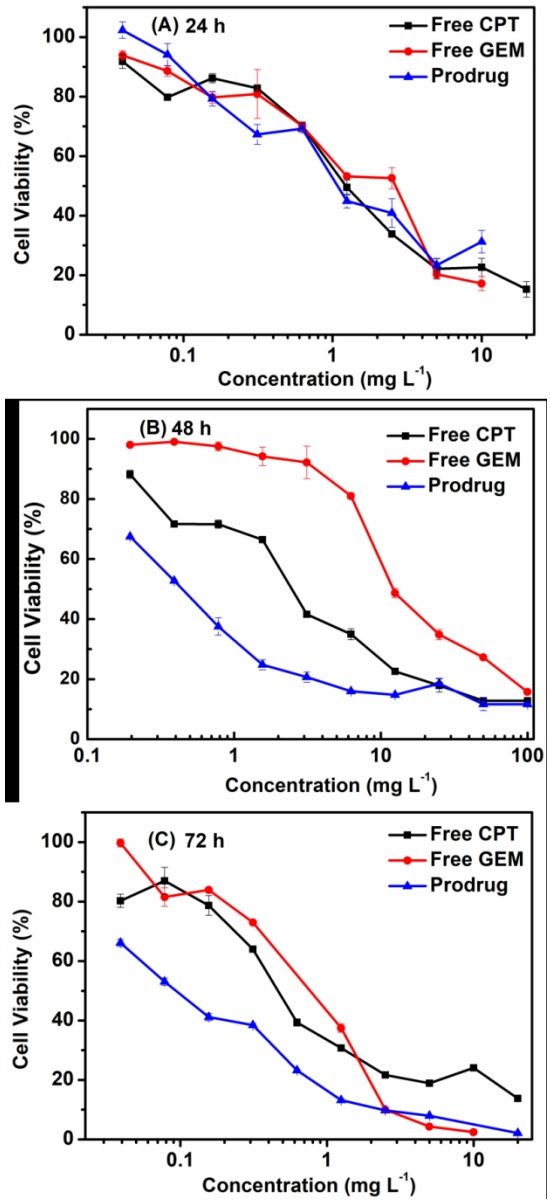

Figure 9. Cell viability of HepG2 cells, treated with CPT-*ss-triazole*-GEM prodrug nanoparticles and free CPT or free GEM with different drug dosages for various different incubation times: (A) 24 h, (B) 48 h and (C) 72 h. The IC50 values of free CPT, free GEM, and CPT-*ss-triazole*-GEM produrg were determined by GraphPad Prism 5 software.

135x299mm (150 x 150 DPI)

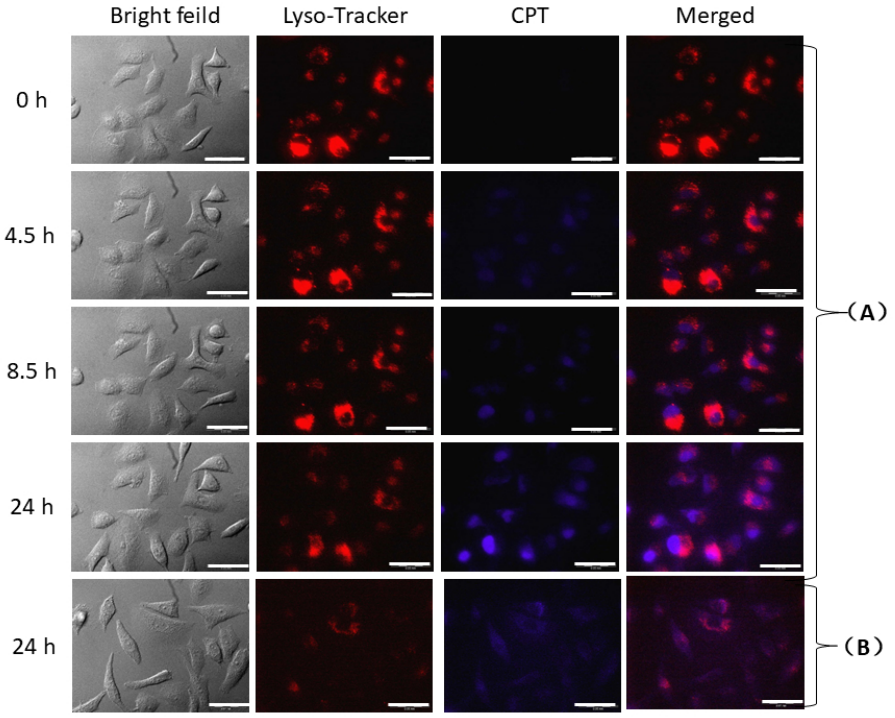

Figure 10. Fluorescence images of HepG2 cells incubated with (A) CPT-*ss*-*triazole*-GEM nanoparticles and (B) free CPT for different times. The CPT dosage was 17.98 mg L^{-1}. For each panel, images from left to right show bright field images, cell nuclei stained by Lyso-Tracker Red (red), CPT (blue) and overlays of the blue and red images. The scale bars are 50 μm in all images.

254x190mm (96 x 96 DPI)

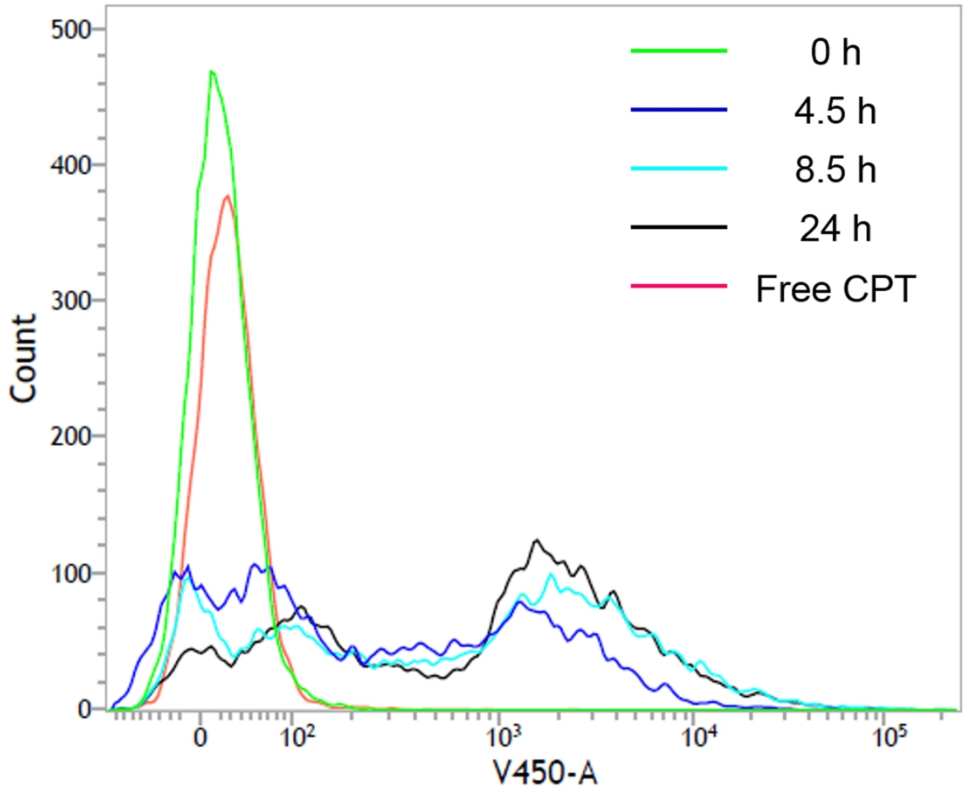

Figure 11. Flow cytometry curves of HepG2 cells treated with CPT-*ss*-*triazole*-GEM prodrug nanoparticles for different times (4.5 h, 8.5 h, and 24 h) with a certain concentration of CPT (17.98 mg L^{-1}).

170x136mm (300 x 300 DPI)

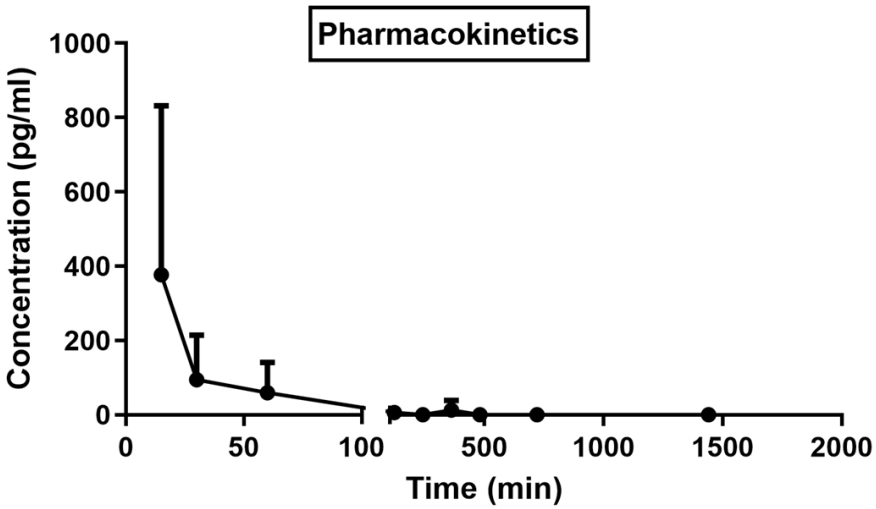

Figure 12. The pharmacokinetic curve of CPT-*ss-triazole*-GEM prodrug. The mice were intravenously administration of CPT-*ss-triazole*-GEM prodrug at dose of 5 mg kg^{-1}. The blood samples were collected at the indicated time point. The validated UHPLC-MS/MS assay was employed to determine the concen-tration of CPT-*ss-triazole*-GEM prodrug. The concentration time curve was plotted, n = 6

312x171mm (96 x 96 DPI)

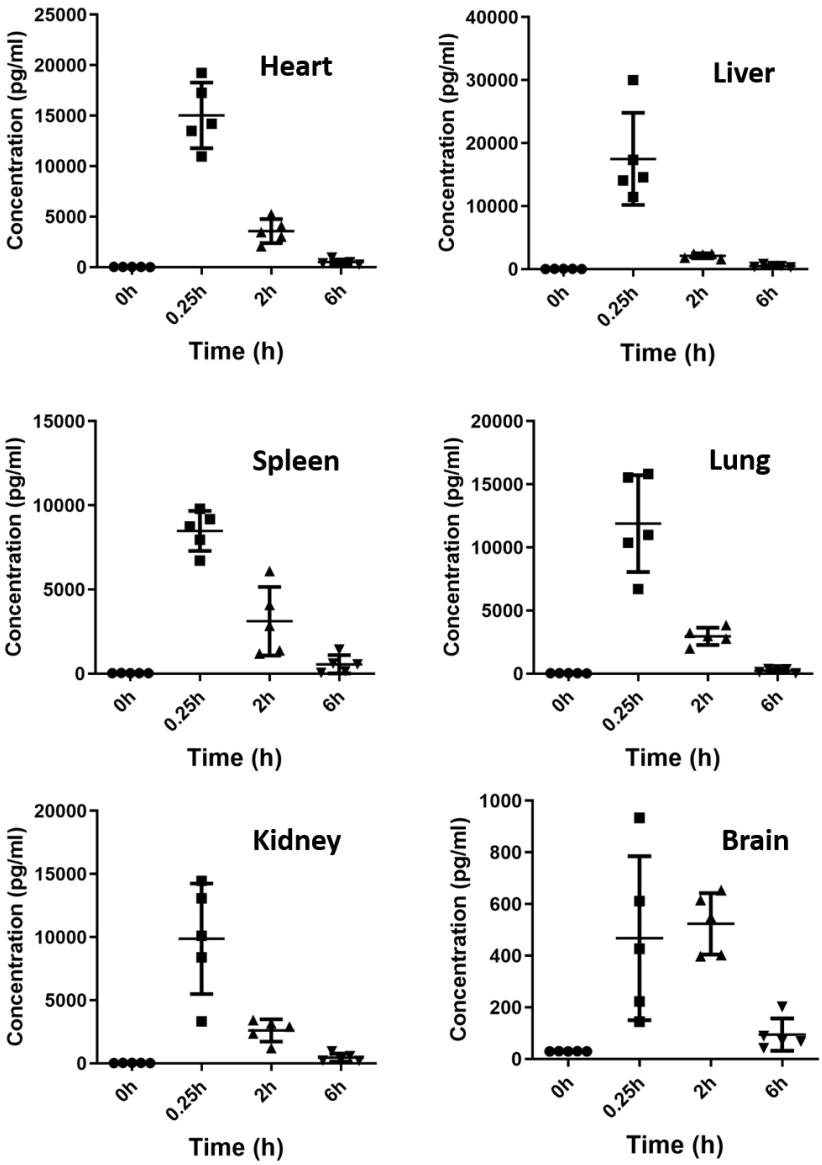

Figure 13. Tissue distribution of CPT-*ss-triazole*-GEM prodrug. The mice were intravenously administration of CPT-*ss-triazole*-GEM prodrug at dose of 5 mg kg^{-1}. The blood, heart, liver, spleen, lung, kidney, brain samples were collected at 0.25 h. The validated UHPLC-MS/MS assay was employed to determine the concentration of CPT-*ss-triazole*-GEM in each organ. The concentration time curve was plotted, n = 6.

171x241mm (150 x 150 DPI)

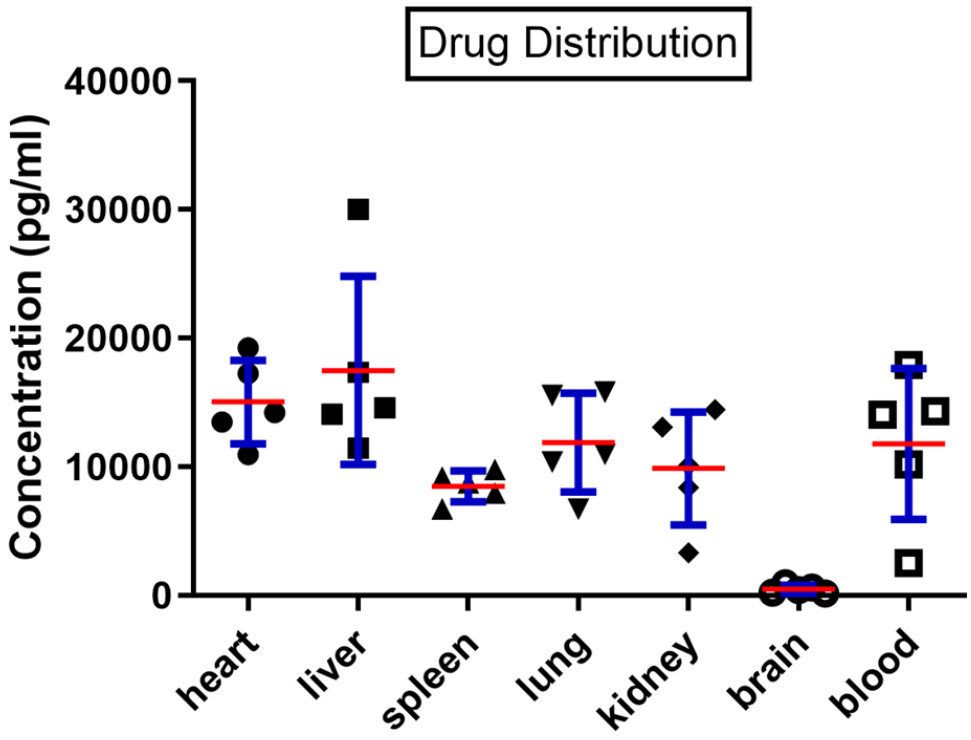

Figure 14. The distribution study of CPT-*ss-triazole*-GEM prodrug. The mice were intravenously administration of CPT-*ss-triazole*-GEM prodrug at dose of 5 mg kg^{-1}. The blood, heart, liver, spleen, lung, kidney, brain samples were collected at 0.25 h. The validated UHPLC-MS/MS assay was used to determine the concentration of CPT-*ss-triazole*-GEM prodrug in each organ. The concentration time curve was plotted, n = 6.

252x188mm (96 x 96 DPI)

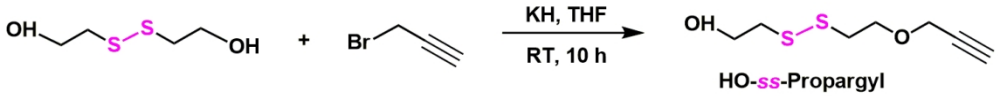

R1. Synthesis of 2-[(2-(2-Propyn-1-yloxy)ethyl)dithio]ethanol.

127x12mm (300 x 300 DPI)

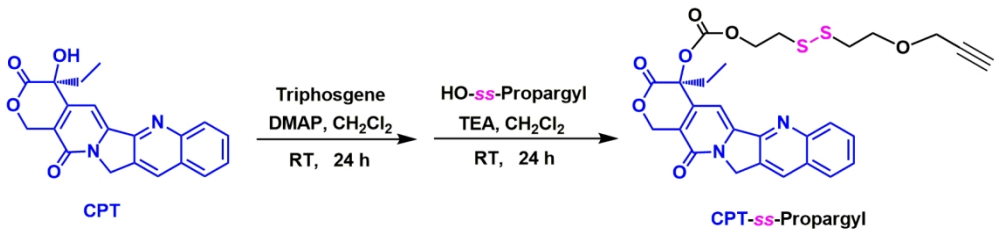

R2. Synthesis of CPT-*ss*-Propargyl.

144x33mm (300 x 300 DPI)

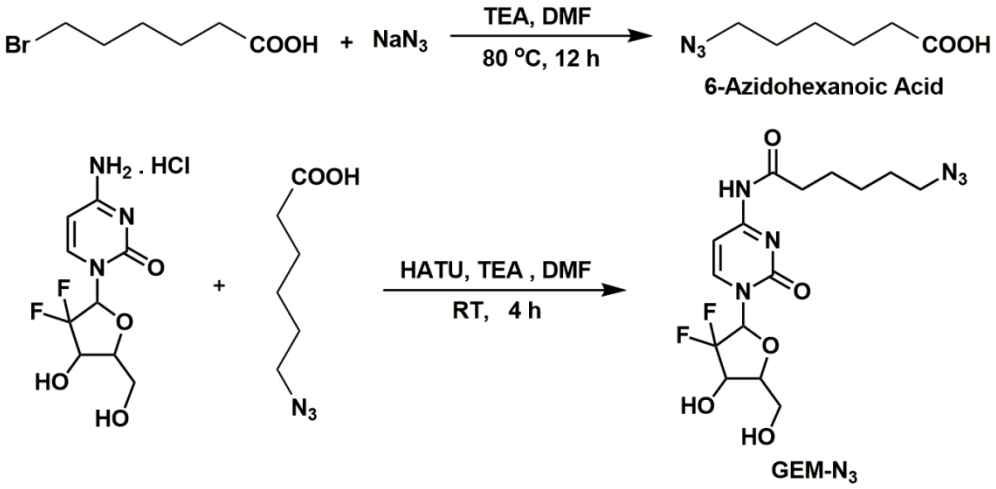

R3. Synthesis of GEM-Azide.

114x55mm (300 x 300 DPI)

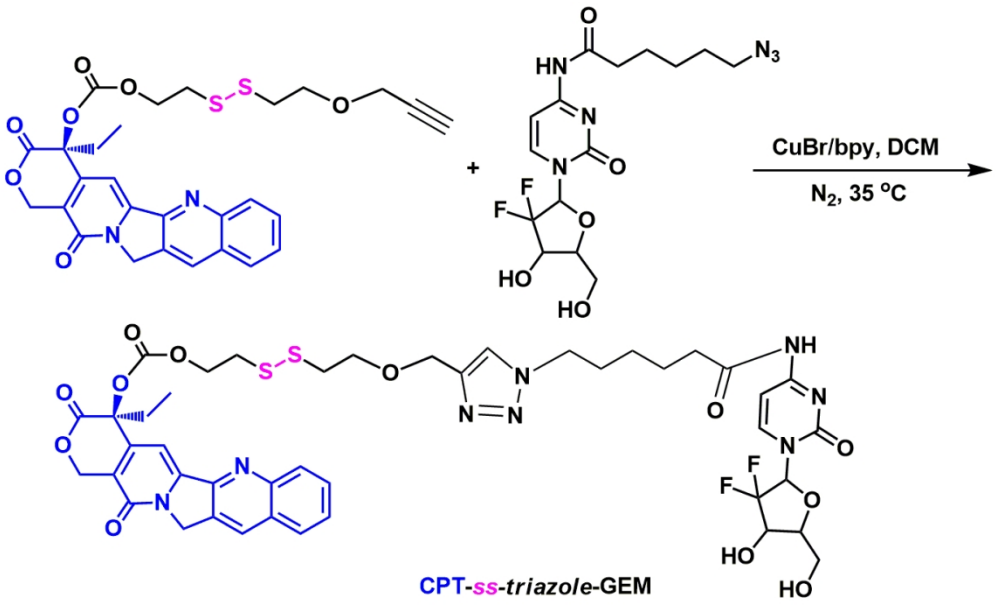

R4. Synthesis of Reduction-Responsive Small Molecule Prodrug CPT-*ss*-*triazole*-GEM.

116x70mm (300 x 300 DPI)